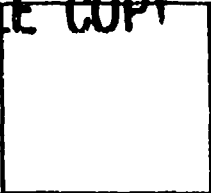


DTIC FILE COPY

PHOTOGRAPH THIS SHEET

AD-A200 129

DTIC ACCESSION NUMBER



LEVEL



INVENTORY

A CORE FACILITY FOR THE STUDY
OF NEUROTOXINS OF BIOLOGICAL ORIGIN

DOCUMENT IDENTIFICATION
15 JUNE 1987

This document has been approved
for public release and sale its
distribution is unlimited.

DISTRIBUTION STATEMENT

ACCESSION FOR	
NTIS	GRA&I <input checked="" type="checkbox"/>
DTIC	TAB <input type="checkbox"/>
UNANNOUNCED	<input type="checkbox"/>
JUSTIFICATION	
BY	
DISTRIBUTION /	
AVAILABILITY CODES	
DIST	AVAIL AND/OR SPECIAL
A-1	

DISTRIBUTION STAMP

"Original contains color
plates: All DTIC reproductions
will be in black and
white"

DTIC ELECTE
OCT 27 1988
S D
GE

DATE ACCESSIONED

Empty box for DATE RETURNED

DATE RETURNED

88 10 20 024

DATE RECEIVED IN DTIC

Empty box for REGISTERED OR CERTIFIED NO.

REGISTERED OR CERTIFIED NO.

PHOTOGRAPH THIS SHEET AND RETURN TO DTIC-DDAC

AD-A200 129

AD _____

A CORE FACILITY FOR THE STUDY OF
NEUROTOXINS OF BIOLOGICAL ORIGIN

Annual Report

June 15, 1987

Lance L. Simpson

Supported by:

U.S. ARMY MEDICAL RESEARCH AND DEVELOPMENT COMMAND
Fort Detrick, Frederick, Maryland 21701-5012

Contract No. DAMD17-86-C-6161

Department of Medicine
Jefferson Medical College
1025 Walnut Street
Philadelphia, Pennsylvania 19107

DOD DISTRIBUTION STATEMENT

Approved for public release; distribution unlimited

The findings in this report are not to be construed as
an official Department of the Army position unless so
designated by other authorized documents.

88 10 20 024

REPORT DOCUMENTATION PAGE

Form Approved
OMB No. 0704-0188

1a. REPORT SECURITY CLASSIFICATION UNCLASSIFIED		1b. RESTRICTIVE MARKINGS	
2a. SECURITY CLASSIFICATION AUTHORITY		3. DISTRIBUTION / AVAILABILITY OF REPORT Approved for public release; distribution unlimited	
2b. DECLASSIFICATION / DOWNGRADING SCHEDULE			
4. PERFORMING ORGANIZATION REPORT NUMBER(S)		5. MONITORING ORGANIZATION REPORT NUMBER(S)	
6a. NAME OF PERFORMING ORGANIZATION Department of Medicine Jefferson Medical College	6b. OFFICE SYMBOL (if applicable)	7a. NAME OF MONITORING ORGANIZATION	
6c. ADDRESS (City, State, and ZIP Code) 1025 Walnut Street Philadelphia, Pennsylvania 19107		7b. ADDRESS (City, State, and ZIP Code)	
8a. NAME OF FUNDING / SPONSORING ORGANIZATION U.S. Army Medical Research & Development Command	8b. OFFICE SYMBOL (if applicable)	9. PROCUREMENT INSTRUMENT IDENTIFICATION NUMBER DAMD17-86-C-6161	
8c. ADDRESS (City, State, and ZIP Code) Fort Detrick Frederick, Maryland 21701-5012		10. SOURCE OF FUNDING NUMBERS	
		PROGRAM ELEMENT NO. 61102A	PROJECT NO. 3M1 61102BS12
		TASK NO. AA	WORK UNIT ACCESSION NO. 138
11. TITLE (Include Security Classification) (U) A Core Facility for the Study of Neurotoxins of Biological Origin			
12. PERSONAL AUTHOR(S) Lance I. Simpson			
13a. TYPE OF REPORT Annual	13b. TIME COVERED FROM 5/15/86 TO 5/14/87	14. DATE OF REPORT (Year, Month, Day) 1987 June 15	15. PAGE COUNT 64
16. SUPPLEMENTARY NOTATION			
17. COSATI CGDES		18. SUBJECT TERMS (Continue on reverse if necessary and identify by block number)	
FIELD	GROUP	SUB-GROUP	
06	15	Neurophysiology Toxin	
06	01	Central nervous system Mechanism	
19. ABSTRACT (Continue on reverse if necessary and identify by block number)			
20. DISTRIBUTION / AVAILABILITY OF ABSTRACT <input type="checkbox"/> UNCLASSIFIED/UNLIMITED <input checked="" type="checkbox"/> SAME AS RPT <input type="checkbox"/> DTIC USERS		21. ABSTRACT SECURITY CLASSIFICATION Unclassified	
22a. NAME OF RESPONSIBLE INDIVIDUAL Mary Frances Bostian		22b. TELEPHONE (Include Area Code) 301-663-7325	22c. OFFICE SYMBOL SGRD-RMI-S

FOREWORD

In conducting the research described in this report, the investigator(s) adhered to the "Guide for the Care and Use of Laboratory Animals," prepared by the Committee on Care and Use of Laboratory Animals of the Institute of Laboratory Animal Resources, National Research Council (DHEW Publication No. (NIH) 86-23, Revised 1985).

Summary

Research has been conducted in three thematic areas, as follows:

- i.) Neurological studies
- ii.) Neuropharmacological and immunological studies
- iii.) Electrophysiological studies

The data that have been obtained fall into six major categories:

- i.) Definitive studies on the central nervous system effects of tetanus toxin.
- ii.) Initial studies on the isolation and characterization of gyroxin
- iii.) Concluding studies on the enzymatic properties of the botulinum binary toxin
- iv.) Continuing studies on the development of a secretory cell that is responsive to most or all of the neurotoxins of interest
- v.) Concluding studies on deltamethrin and sodium channels in nerve cells grown in culture
- vi.) Continuing studies on ryanodine and calcium flux in excitable tissues

TABLE OF CONTENTS

FOREWORD	1
SUMMARY	2
TABLE OF CONTENTS	3
I. NEUROLOGICAL STUDIES	4
A. Tetanus Toxin	4
B. Gyroxin	10
II. NEUROPHARMACOLOGICAL STUDIES	18
A. Botulinum Binary Toxin	18
B. Morphology and Messenger Correlates	30
III. ELECTROPHYSIOLOGICAL STUDIES	
A. Pyrethrins	40
B. Ryanodine	48
DISTRIBUTION LIST	61

I. Neurological Studies

A. Tetanus Toxin

Specific Aims

The aims of this research were:

(1) To determine the effect of intramuscular injection of tetanus toxin on the local cerebral metabolic rate for glucose (LCMRg) in the rat. In humans demonstrating tetanus poisoning, there is extreme anxiousness and disinhibition of motor systems both at the spinal and supraspinal levels. The nuclei and pathways that mediate this response are unknown. The major systems that were surveyed included: (1) the intralaminar and reticular nuclei of the thalamus; (2) the major components of the thalamo-cortical motor circuits; (3) the meso-cortical dopaminergic limbic system; (4) brain stem nuclei; and (5) reticular formation at midbrain, pontine, and medullary levels.

Methods (Tetanus)

Thirty-two adult male Long Evans hooded rats were used during this period. Twelve rats were used to determine the survival time of these animals to tetanus toxin. Four groups of three animals were injected with 1.0, 0.1, 0.01, 0.001 micrograms of toxin i.m. in the left rear limb.

Twenty rats, weighing 300-400 gms each, were employed for the metabolic study. Fifteen animals were injected with 0.001 ug tetanus toxin into the left rear limb. Five animals were sacrificed at 24 hrs, 5 at 48 hrs and 5 at 72 hrs following toxin injection. Five animals not injected with toxin were used as controls.

The animals were housed in wire hanging cages, adapted to a light:dark cycle LD 10.5:13.5 (lights on 0600h), and supplied with food and water ad libitum. Each rat was fasted for a minimum of 12 h before surgical preparation. On the day of the experiment, rats were anesthetized lightly with an intramuscular injection of Ketamine (40 mg/kg) and Acepromazine (1 mg/kg) for the placement of femoral venous and arterial catheters (PE 50 tubing, Clay Adams). Isotonic heparinized saline was infused continuously through the catheters at 0.1 ml/h to maintain patency. After surgery, animals were restrained passively in clear, plexiglass holders (Fisher Scientific) while recovering from anesthesia for a minimum of 5 h.

During recovery from anesthesia and for the remainder of the experiment, the rats were exposed to a steady level of light and sound. The light irradiance at the level of the animals' eyes was 100 ± 2 uW/cm². Light irradiance was measured with a J16 Radiometer/Photometer with a J6512 Microwatt Probe (Tektronix, Inc., Beaverton, OR). The sound was provided by a white noise generator (Model 455, Grason-Stradler) and dual speakers (3 1/2" Realistic) with flat sound production from 70 to 15,000 Hz. The sound level was set to 80 db and was modified only slightly (2-5 db) by external laboratory sounds. Sound levels were measured with a Precision Sound Level Meter (Type 2203, Bruel and Kjoer).

At the start of the metabolic study, the rats received a bolus injection of ¹⁴C-2-deoxyglucose (100 uCi/kg body weight) in 1 ml physiologic saline through the femoral vein catheter. Four or five arterial blood samples (0.1-0.2 ml each) were taken during the first five minutes after 2DG injection. Additional arterial blood samples were taken at 5 minute intervals for the remainder of the study.

Forty-five minutes after the 2DG injection, the animals were sacrificed with an intravenous overdose of sodium pentobarbital. The spinal cords were removed rapidly and frozen in isopentane cooled with dry ice to -40°C . The blood samples were centrifuged (3,000 RPM) at 4°C for 20 minutes. Duplicate 20 μl samples of plasma were pipetted into scintillation vials containing 10 ml of aqueous counting scintillant (Amersham, Arlington, IL). Samples were vortexed, placed in a scintillation counter (Tracor Analytic, Elk Grove, IL) to determine ^{14}C levels. Plasma glucose concentrations also were determined in each sample. Ten μl of plasma were added to 1 ml glucose reagent (SVR) (Calbiochem-Behring, La Jolla, CA) and read on a Gilford spectrophotometer Model 20 (Oberline, OR).

Each cord/brain was sectioned serially in 20 micron sections at -12° on an American Optical Cryostat (Model 855, Buffalo, NY). The sections were placed on glass slide and dried on a warming plate at 42°C . The slides then were exposed along with plastic ^{14}C standards (Amersham) on X-ray film (Kodak, SB-5) for 5-7 days at room temperature. After exposure, the film was developed and the spinal cord sections were fixed over formalin fumes before staining with thionin. The Rexed layers of each section was identified using the Paxinos and Watson stereotaxic atlas of the rat. The tissue ^{14}C concentration was determined using a computerized image-processing system (Alexander and Schwartzman, 1984). At each level, the isotope concentration of each layer was computed bilaterally. The mean concentration from three consecutive sections was used to minimize section thickness variations. The local spinal metabolic rate for glucose (LSMRg) was calculated quantitatively from the tissue isotope concentration and the arterial deoxyglucose and glucose curves.

The rate and lumped constants used were those evaluated for the rat (Sokoloff et al., '77). The numerical value for LSMRg is in micromoles of glucose per 100 grams of tissue per minute.

Results (Tetanus)

The survival times of animals injected with tetanus toxin is shown in Table I. We chose the 0.001 dose because it allowed for the study of the effect of this toxin at different stages of symptomatology. At 24 hrs the animals were asymptomatic, at 48 hrs the animals demonstrated paralysis of the rear right limb, and at 72 hrs they were hemiparetic.

The results of the 2-deoxyglucose experiment in seven animals (2 at 24 hrs, 3 at 48 hrs and 2 at 72 hrs) are tabulated in Tables II, III and IV. The 24 hr animals demonstrated no changes in LSMRg at the cervical and thoracic levels. At the lumbar level all Rexed layers were depressed. At 48 and 72 hrs following toxin injection, Rexed layers I, II and III, the medial segment of layers V and VI and layers VII, VIII and IX were depressed at the cervical and lumbar levels. The thoracic cord was unchanged. In the remaining eight animals, the spinal cords have been cut, plated on x-ray film and developed. The evaluation of the LSMRg in the different Rexed layers is currently in progress.

The early changes in spinal glucose metabolism were restricted to the lumbar area. This is not surprising since the injection was in the rear limb. At the late stages, the metabolic changes had spread and involved the cervical cord. In

Table I

<u>Toxin Dose</u>	<u>Survival Time</u>
1.0	8-12 hours
0.1	20-24 hours
0.01	38-44 hours
0.001	92-104 hours

- (1) The toxin dose is in micrograms.
- (2) The animals were injected i.m. in the left hamstring.

Rexed Layers

Table II

Local Spinal metabolic rate for glucose in the cervical cord of tetanus injected rats.

	Controls		24 hours		48 hours		72 hours	
	R	L	R	L	R	L	R	L
I	38.9	39.6	38.1	37.5	30.4	31.0	32.0	31.4
II	42.4	46.6	36.0	42.3	34.2	32.0	31.9	34.3
III	44.2	50.0	42.9	43.4	39.5	36.9	37.1	36.9
IV	48.7	53.0	41.7	44.9	48.6	44.2	43.2	41.7
V L/M	49.1/50.4	55.0/59.8	43.8/56.1	48.6/52.9	48.8/49.8	42.7/48.5	48.5/49.5	44.5/51.4
VI L/M	51.0/59.4	53.9/61.1	46.9/59.1	51.5/56.3	51.8/51.4	48.4/49.4	48.6/53.00	44.6/50.1
VII	58.4	58.2	52.3	53.3	54.8	50.3	49.3	49.4
VIII	54.1	53.9	50.5	42.3	49.3	43.6	45.7	41.9
IX	52.2	51.3	44.0	43.9	48.3	44.2	44.3	43.5
X		54.5		53.5		48.4		50.6

Table III

Local spinal metabolic rate for glucose in the thoracic cord of tetanus injected rats.

Rexed Layers	Control		24 hrs		48 hrs		72 hrs	
	R	L	R	L	R	L	R	L
I	35.9	35.4	34.1	36.3	32.5	36.5	32.0	31.4
II	34.6	35.4	34.3	36.0	33.4	33.8	33.2	33.8
III	34.9	35.7	37.5	38.1	34.8	35.8	37.4	38.6
IV	38.2	38.4	42.5	41.8	38.0	37.6	40.9	40.2
V	40.7	41.1	42.5	43.5	38.5	39.6	42.0	42.0
VII	42.8	42.7	45.1	44.6	43.8	43.5	47.8	44.1
VIII	40.8	41.8	39.9	40.2	38.5	38.9	41.8	41.8
IX	37.2	41.8	38.8	36.9	37.5	38.5	38.1	38.2
IXL	33.6	34.7	37.3	32.1	44.9	41.0	35.9	36.9
X		41.5		37.7		39.2		42.8

Rexed Layers

Table IV

Local spinal metabolic rate for glucose in the lumbar cord of tetanus injected rats.

	Controls		24 hours		48 hours		72 hours	
	R	L	R	L	R	L	R	L
I	42.0	44.8	30.8	32.8	36.4	38.7	38.4	41.2
II	44.4	42.5	35.4	33.7	37.5	39.7	41.8	43.4
III	46.9	44.8	37.0	36.6	37.7	38.9	40.4	47.0
IV	48.9	47.6	38.9	38.9	38.8	41.5	47.6	49.3
V L/M	51.8/60.7	52.0/62.6	41.2/46.0	40.6/44.6	43.8/45.0	44.1/48.2	50.0/54.1	53.3/59.8
VI L/M	53.9/60.8	55.0/62.1	40.9/45.9	43.9/47.9	44.4/46.8	46.9/51.8	50.0/58.1	51.5/60.0
VII	57.2	56.4	41.8	42.5	45.4	44.1	37.6	37.8
VIII	54.4	50.8	37.3	36.3	41.3	40.7	44.9	46.7
IX	51.7	52.0	38.7	36.1	40.4	40.0	46.9	45.4
X		54.1		44.6		49.9		58.8

general the sensory layers of the cord (dorsal) were more involved than the motor layers.

Forty central nervous system structures were analyzed utilizing the quantitative 2-deoxyglucose technique. There was no significant difference of glucose utilization in any structure between control and experimental groups (Table VI). However, several animals showed somatotopic differences within specific nuclei. These changes were most evident in the motor cortex, the caudoputamen, globus pallidus, and VPL of the thalamus. These structures are intimately involved in sensorimotor systems. All of these somatotopic changes were noted contralateral to the injected extremity. These changes are illustrated in Figure 1.

Although these experiments demonstrate that the tetanus toxin does not appear to have specific central nervous system (CNS) effects, it may be utilized to map specific central nuclei by paralyzing specific muscles. We can then survey for changes of CNS metabolism in the central connections of these peripheral structures.

n. Gyroxin

Specific Aims

The aims of this project were:

- (1) To isolate the gyroxin protein from the venom of the South American rattlesnake Crotalus durissus terrificus and the Central American rattlesnake Crotalus durissus durissus.

Table VI. Local Cerebral Metabolic Rate for Glucose in Tetanus Injected Rats

	Control (N=5)	48 hours (N=5)	72 hours (N=5)
Thalamus			
AV	102.6 ± 2.27	100.4 ± 4.95	102.1 ± 3.02
PVA	79.5 ± 6.04	73.7 ± 2.75	74.5 ± 2.68
VL	81.2 ± 2.67	86.8 ± 2.87	87.7 ± 1.77
VPL	69.8 ± 1.47	72.8 ± 2.35	71.7 ± 2.13
UPM	72.8 ± 2.01	73.6 ± 2.54	72.8 ± 2.02
MD	93.2 ± 2.47	98.2 ± 3.28	91.9 ± 3.65
Re	71.4 ± 3.44	71.8 ± 1.27	71.0 ± 5.74
CM	79.2 ± 2.65	73.0 ± 2.11	74.5 ± 3.19
PO	82.1 ± 2.31	86.7 ± 2.91	79.6 ± 1.99
Medial geniculate	102.4 ± 1.05	101.0 ± 3.17	100.7 ± 2.78
Lateral "	86.6 ± 4.16	87.6 ± 5.71	87.6 ± 4.05
Habenula	102.2 ± 2.40	119.5 ± 3.65	108.3 ± 2.61
Periaqueductal grey	60.3 ± 2.43	62.0 ± 0.63	62.5 ± 4.20
Sup Colliculus layers U 1-3	84.1 ± 2.45	83.0 ± 3.82	84.9 ± 1.70
L 4-6	78.4 ± 3.47	78.0 ± 3.20	78.6 ± 2.30
Inf Colliculus	193.3 ± 5.41	166.0 ± 5.54	175.2 ± 4.04
Nuc Solitarius	50.1 ± 1.59	50.7 ± 1.35	56.8 ± 2.18
Ret Formation PN _O	50.3 ± 0.64	50.4 ± 0.54	51.1 ± 1.71
PN _C	49.2 ± 0.47	49.5 ± 1.23	52.4 ± 1.42
Olfactory Cortex	98.2 ± 1.96	95.1 ± 1.74	104.9 ± 2.05
Frontoparietal motor	100.6 ± 2.31	100.2 ± 1.07	101.5 ± 2.08
sensory	105.8 ± 2.16	102.2 ± 3.42	106.3 ± 2.03
Cingulate Cortex	108.1 ± 6.35	110.8 ± 2.78	104.6 ± 3.41
Auditory Cortex	118.7 ± 1.32	126.7 ± 4.87	119.7 ± 3.20
Visual Area 18	101.5 ± 5.48	103.7 ± 3.26	103.0 ± 2.31
17	105.4 ± 5.21	106.6 ± 4.40	104.6 ± 5.37
Nuc Acc	74.6 ± 2.16	70.4 ± 2.73	78.6 ± 1.95
Olf tubercle	85.1 ± 3.98	81.6 ± 4.34	83.5 ± 2.47
Caudoputamen T	102.4 ± 3.58	101.7 ± 1.92	101.3 ± 1.68
B	94.7 ± 3.43	91.9 ± 2.26	93.9 ± 1.51
Globus pallidus	55.4 ± 2.76	59.2 ± 1.29	53.8 ± 2.22
RN	69.3 ± 1.54	70.6 ± 2.33	72.0 ± 1.51
STN	77.6 ± 0.99	80.4 ± 1.31	80.6 ± 3.28
SN _R	48.5 ± 0.81	51.0 ± 21.9	46.6 ± 0.56
SN _C	62.0 ± 2.07	65.6 ± 1.19	66.0 ± 1.50
Lateral Septum	64.2 ± 2.40	58.5 ± 1.94	58.2 ± 1.38
Medial Septum	77.2 ± 3.55	72.0 ± 3.25	81.7 ± 0.91
Diag Band Brocca	82.3 ± 2.58	72.4 ± 2.49	80.5 ± 1.93
VTA	66.4 ± 1.12	63.0 ± 2.52	61.0 ± 2.04
Hypothalamus			
AHY	54.3 ± 1.80	56.3 ± 3.68	52.6 ± 1.40
VMH	56.7 ± 3.74	53.5 ± 3.82	47.9 ± 1.42
DMH	57.7 ± 2.58	57.6 ± 2.93	56.1 ± 1.86

1. Rats were injected i.m. with 0.001 ug of toxin.
2. The 24 hour group is not completed. There are no differences in lCMRG in the 2 animals evaluated to date.

RIGHT

LEFT

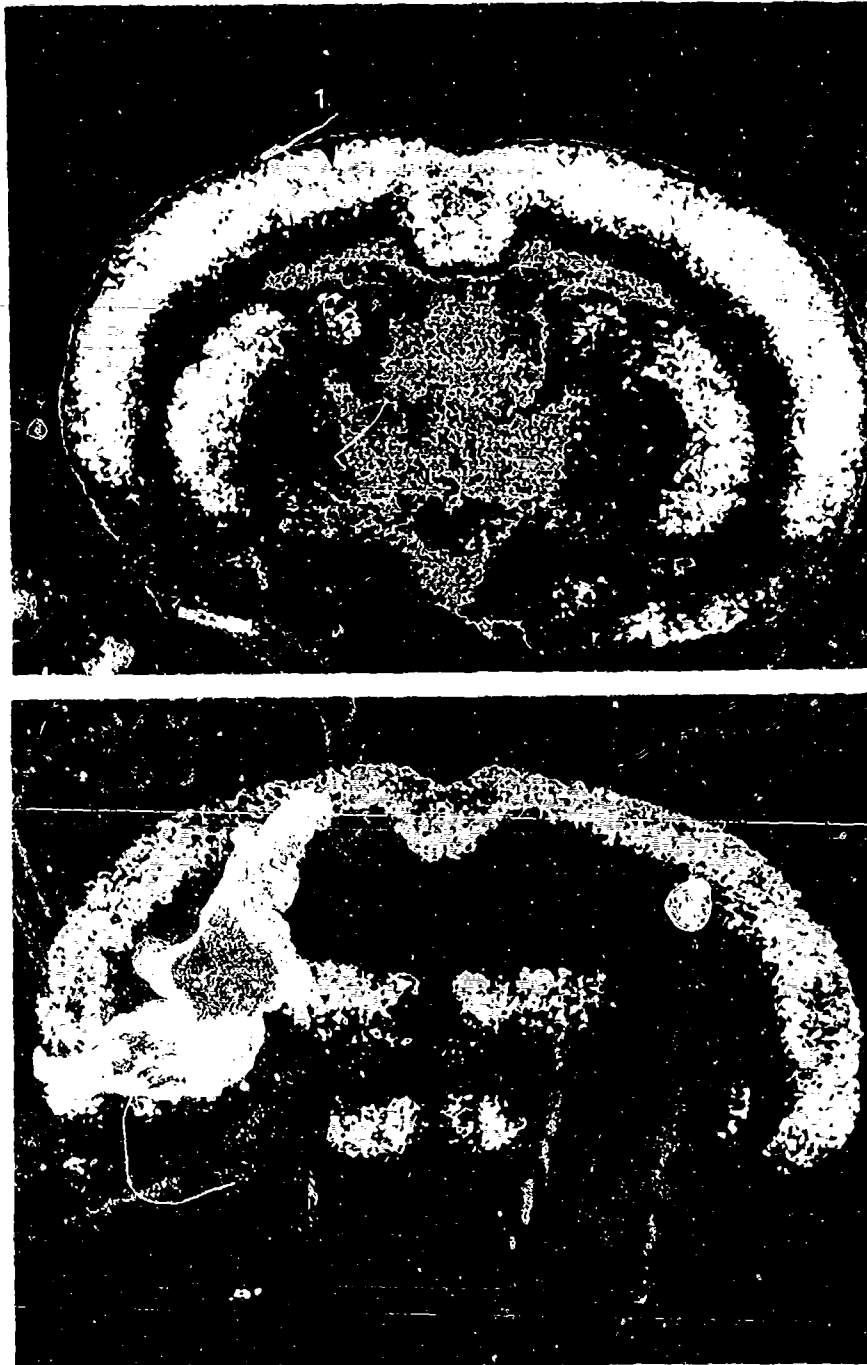


Figure 1. Pseudocolor-coded autoradiograms of a 72 hour tetanus injected rat. Note the relative increase in ICMrg of the right motor cortex (1), caudoputamen (2), globus pallidus (3), and VLM of the thalamus (4).

-45-

(2) To analyze the metabolic effect of gyroxin (a component of rattlesnake venom) on the lCMRg of mice. This protein was isolated by Dr. Alexander using the method of Seki et al. (1980).

Methods (Gyroxin)

Two methods were used for the isolation of gyroxin from the venom of Crotalus durissus terrificus. The first procedure (Barrio, 1961) removes the gyroxin activity from the lethal crotoxin using a one column step gradient procedure on the cation exchange resin Amberlite IRC-50 (Sigma Chemical Co., St. Louis, MO). The gyroxin-containing fraction from this method has good activity, but there is still too much contamination of the sample with crotoxin. Mice injected with this fraction intravenously (tail vein) show the symptoms of gyroxin poisoning (loss of equilibrium, rolling movements and inability to right themselves) but die within a few hours, indicating the presence of significant contamination from the lethal components of the venom.

The purification procedure used most recently is the one described by Seki et al (1980). This procedure uses four column chromatographic steps. The first two steps are identical runs on Sephadex G-75 (Sigma Chemical Co., St. Louis, MO) in which the gyroxin-containing fractions from the first run are pooled, concentrated, then rerun on the same column. The active fractions are pooled and run on a cation exchange column. The active fractions from this are pooled, concentrated and chromatographed on G-75 again.

We have done preliminary semi-quantitative [^{14}C]-2-deoxyglucose (2-DG) experiments with Balb/C mice.

Fifty micrograms of protein from the middle fraction of gyroxin activity (first G-75 column) along with 3uCi of [¹⁴C]-2-deoxyglucose was injected into 18 gm mice via the tail vein. This dose produced the gyroxin syndrome in these mice and did not cause death within the time course of the experiment (indicating little, if any contamination from crotoxin).

The mice were sacrificed by decapitation 45 minutes after injection and the brains were removed and frozen in isopentane cooled to -40°C with dry ice. The brains were stored at -70°C and later cut in 20 um sections, dried and plated on X-ray film (Kodak, SB-5).

Results (Gyroxin)

The first G-75 Sephadex run had gyroxin actively centered around fraction number 50 for both the C.d. terrificus and C.d. durissus rattlesnakes (Figure 1). This fraction produced loss of equilibrium, inability to right themselves and a broad-based gait, but within a day the animals died, indicating contamination by lethal components of the venom (probably crotoxin). The active fractions from the second G-75 run produced the gyroxin syndrome in mice. We also injected rats and the animals demonstrated loss of balance and a broad-based gait. The response was much less pronounced in the rats than in the mice. At this point in the purification, animals injected with the active fraction survived for 4 days, indicating much less contamination with the lethal components of the venom. The active component from the cation exchange column exhibited much higher gyroxin activity per unit protein (0.25 ug protein/gram). Animals injected with this fraction survived indefinitely.

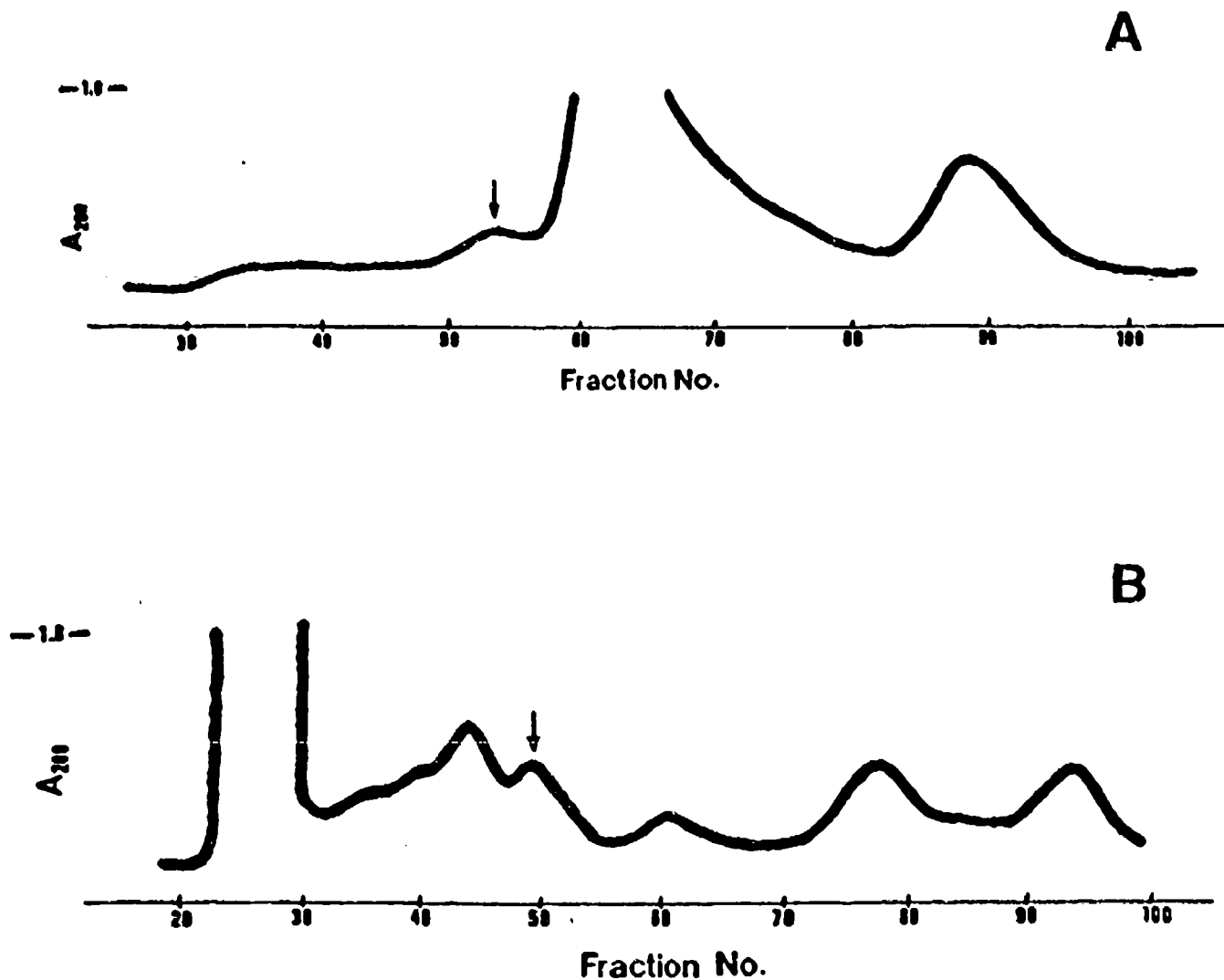


Figure 1. Size exclusion chromatography of *Crotalus* venoms in Sephadex G-75. Chromatography of 200 mg (in 5ml volume) of lyophilized venom from *Crotalus durissus terrificus* (A) and *Crotalus durissus durissus* (B). Gyroxin activity was found in the peaks designated by the arrows.

A squirrel monkey was injected with 300 ug of protein from this fraction and the monkey demonstrated the gyroxin syndrome. Within 1 minute of injection, the animal started to lick his lips and retch. At 2 minutes, the animal lost its balance, fell and could not right itself (Figure 2-a). Fifteen minutes following injection, it could sit broad-based (Figure 2-b). Two hours following injection, the animal appeared normal and was able to balance itself on a perch (Figure 2-c).

The work with gyroxin has importance from a basic science standpoint in that it is a neurotoxin with a profound CNS effect. From a more applied standpoint there is the potential for gaining insight into the mechanisms of spatial disorientation and/or motion sickness.

To date, one control and one mouse injected with partially purified toxin have been prepared. The semi-quantitative 2-deoxyglucose method in these animals has demonstrated dramatic changes both in the vestibular system and in the brain as a whole.

The gyroxin syndrome has been produced in one squirrel monkey. It appears to be reversible. Evaluation of the metabolic changes in central nuclei (cerebellum, vestibular nuclei) may give new insight into basic mechanisms underlying vertigo.

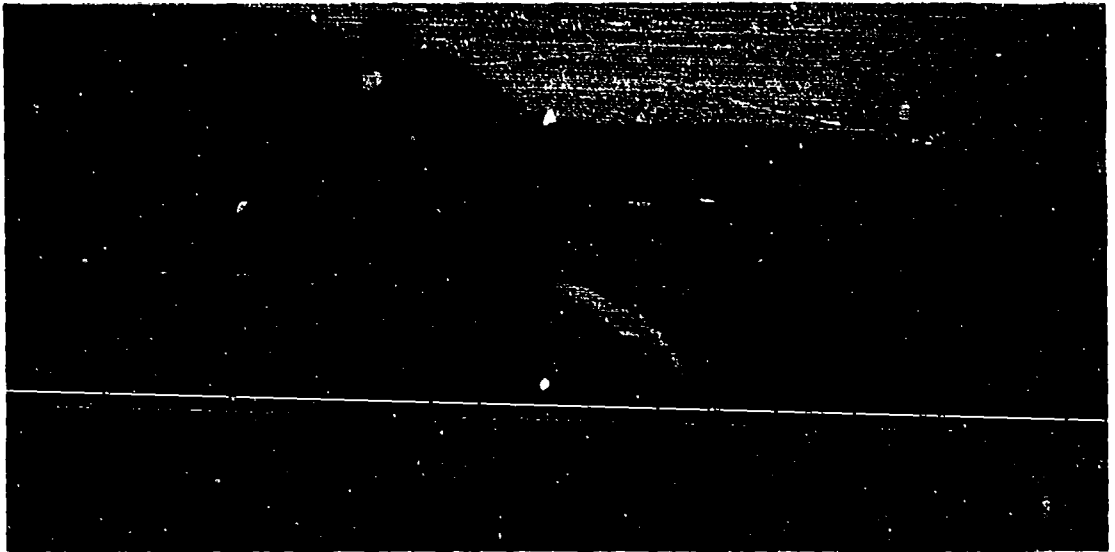
References:

Sokoloff L, Reivich M, Kennedy C et al: The ¹⁴C deoxyglucose method for the measurement of local cerebral glucose utilization. J Neurochem 28:897-916, 1977.

a



b



c



Figure 2. Squirrel monkey (*Saimiri sciureus*) after a 300 ug protein injection of purified gyroxin. (a) 2 minutes after injection, (b) 15 minutes after injection, and (c) 2 hours after injection.

Alexander GM and Schwartzman RJ: Quantitative computer analysis of autoradiographs utilizing a charge-coupled device solid state camera. *Neuroscience Methods* 12:29-36, 1984.

Barrio, A (1961), "Gyroxin, a new Neurotoxin of *Crotalus durissus terrificus* venom", *Acta Physiologica Latinoamericana*, 11, 224.

Seki, C., Vidal, J.C. and Barrio A., (1980), "Purification of Gyroxin from a South American Rattlesnake (*Crotalus durissus terrificus*) Venom", *Toxicon*, 18, 235-247.

II. Neuropharmacological Studies

A. Botulinum Binary Toxin

Specific Aims

The goals are to determine the structure-function relationships of various protein toxins. This means an initial effort to identify enzymatic activity in certain toxins and a subsequent effort to characterize the properties of the enzyme. This report represents the final effort to identify and characterize the enzymatic activity of the botulinum binary toxin.

Methods

Radioisotope assay for ADP-ribosylation. Homo-poly-L-arginine (10 mg/ml) was suspended in dimethylglutaric acid buffer (100 mM, pH 7.0) that contained 5 μ Ci 3 H-NAD, plus other ingredients as indicated under Results. The reaction volume was 100 μ l, the incubation temperature was 33°C and the length of incubation was 1 hour, unless otherwise indicated. At the end of incubation, the mono(ADP-ribosyl)ated polyarginine was precipitated by adding phosphate buffer (1 ml, 100 mM, pH 7.0). The mixture was centrifuged at 4,500 x G, and the pellet was washed three times. The final pellet was dissolved in 0.5 ml of 1.0 mM HCl, followed by 1.0 ml of 100 mM dimethylglutaric acid buffer (pH 7.0). An aliquot of the resuspended material was added to a scintillation cocktail, and the radioactivity was quantified by liquid scintillation spectrometry. Experimental values were corrected by subtracting background

activity in solutions without enzyme. Assays were performed in duplicate, and each experiment was done at least twice.

High performance liquid chromatography assay for mono(ADP-ribosylation). The reaction conditions were the same as those described above. At the end of incubation, samples were injected into an LKB Gti HPLC system. A gradient was created by using 20 mM Tris-HCl, pH 8.0, and 50 mM Tris-HCl, pH 8.0, containing 1M NaCl. The technique allowed for resolution of NAD, nicotinamide and ADP-ribose. The elution times were: NAD, ~ 6 minutes; nicotinamide, ~ 10 minutes; and ADP-ribose, ~ 21.5 minutes.

RESULTS

Assay for enzyme activity. Mono(ADP-ribosylation) is typically assayed by two techniques: incorporation of an ADP-ribose group into substrate or release of a free nicotinamide group. Time and concentration-dependent incorporation of labeled ADP-ribose into polyarginine has previously been reported for the catalytic chains of binary toxins. The binary toxin from Clostridium botulinum also produces time and concentration-dependent release of nicotinamide (Figure 1).

The light chain of the binary toxin ($10^{-8}M$) was incubated with $^3H(2,4\text{-nicotinamide})NAD$ in the presence of polyarginine. At the end of various times, the reaction mixture was injected into the HPLC. Unreacted NAD emerged at approximately 6 minutes, and it was essentially homogeneous nucleotide. NAD that was reacted with toxin in

the presence of substrate was converted to free nicotinamide. The ADP-ribose moiety attached to polyarginine eluted in the void volume.

The data indicate that mono(ADP-ribosyl)ation by the Clostridium botulinum binary toxin can be detected either by monitoring the incorporation of adenine labeled material into substrate or by monitoring the liberation of nicotinamide labeled material. Therefore, both methods have been used, depending on which was more appropriate for a particular experiment.

pH Optimum. Enzyme activity was assayed in dimethylglutaric acid buffer and in boric acid-citric acid-phosphate buffer. The former has an effective buffer range from about pH 4.0 to 8.0. The latter is an effective buffer from pH 2.0 to 12.0.

Enzyme activity was assayed by monitoring the incorporation of ADP-ribose into polyarginine. Maximal activity for both buffers was obtained in the pH range of 7.0 to 8.0 (Figure 2). Although the shapes of the curves were the same for both buffers, the absolute values were slightly different. Enzyme activity was approximately 20% higher in the dimethylglutaric acid buffer.

Exposure of the enzyme to low pH for short periods of time did not produce irreversible loss of activity. The enzyme ($10^{-8}M$) was incubated in DMG buffer (pH 5.0) for thirty minutes, after which pH was adjusted to 7.0, polyarginine was added and adenine-labeled NAD was provided.

Compared to enzyme that had been maintained at pH 7.0, enzyme that had been exposed to low pH and then adjusted to 7.0 possessed 85 to 90 percent of its original activity (two assays done in duplicate).

Effects of physiological salts. Calcium, magnesium, sodium and potassium were tested for their ability to alter the activity of the enzyme ($10^{-8}M$). All four cations exerted an inhibitory effect (Figure 3). The divalent cations were more effective than the monovalent cations, but the difference could not be explained solely on the basis of charge. The IC50 for the divalent cations was approximately 25 mM, and the IC50 for the monovalent cations was approximately 160 mM. It should be pointed out that the inhibitory effect was not due simply to increased tonicity. The presence of 33 mM calcium in a 100 mM dimethylglutaric acid buffer produced greater than 50% inhibition of enzyme activity. When dimethylglutaric acid was increased to 133 mM in the absence of calcium, there was negligible inhibition (<10%) of enzyme activity.

In addition to assays done in the absence of added cation, experiments were also done in the presence of EDTA (1 mM). This chelator had no effect on enzymatic activity (two assays done in duplicate).

Enhancement of enzyme activity. The light chain of the binary toxin ($10^{-8}M$) was incubated with adenine labeled NAD and polyarginine. The incorporation of ADP-ribose was measured in the presence of various concentrations of

histone and lysolecithin. Both substances produced concentration-dependent enhancement of enzyme activity (Figure 4). ADP-ribosylation was enhanced almost twofold.

Antagonism of enzyme activity. Several agents that are known to be inhibitors of mono(ADP-ribosylation) were tested for their effects on the binary toxin. When tested at 10^{-1} M, nicotinamide, thymidine, theophylline and histamine all produced substantial inhibition. The respective values (percent inhibition; two assays done in duplicate) were: nicotinamide, 84 ± 4 ; thymidine, 61 ± 7 ; theophylline, 85 ± 8 ; and histamine, 91 ± 3 .

Dithiothreitol was tested both for its ability to reduce enzyme activity and for its ability to reduce any intrachain disulfide bonds. When the enzyme was exposed to the reducing agent (50 mM) for 30 minutes at pH 7.0, residual biological activity was between 90 and 100 percent of control values. When the treated enzyme was submitted to SDS-PAGE, it migrated as a single band that was not distinguishable from the native protein. When the enzyme was exposed to larger amounts of DTT (250 mM) there was some inhibition of catalytic activity (~ 30 percent), but the protein still migrated as a single band in SDS-PAGE.

Denaturation of the enzyme. The botulinum binary toxin was heat sensitive. When the enzyme was boiled (three assays done in duplicate), it lost 80 percent or more of its activity within 1 minute. When the enzyme was exposed to a temperature of 50°C , it lost 50 percent of its activity

within 5 minutes. When the enzyme was exposed to 30° C, it lost less than 10 percent of its activity within 100 minutes.

Both 2M urea and 6M guanidine HCl caused loss of enzymatic activity, but the effect was somewhat reversible. For example, when the enzyme (10^{-8} M) was exposed to the denaturing agents for 30 minutes, then repeatedly washed and filtered (Centricon 10, Amicon Corp., Danvers, MA) with dimethylglutaric acid buffer (pH 7.0), the residual activity was substantial. Enzyme treated with 2M urea (2 assays in triplicate) possessed 48 percent of control activity, and enzyme treated with 6M guanidine HCl (2 assays in triplicate) had 63 percent of control activity.

Lysosomal proteases. The light chain of the toxin (10^{-8} M) was exposed individually or collectively to four lysosomal proteases: cathepsin B, cathepsin H, catheptic carboxypeptidase B and dipeptidyl aminopeptidase. Assays were done at pH 5.0 and at pH 7.0, either in the absence or presence of dithiothreitol (20 mM). Each of the proteases was tested at a concentration of 10 g per 100 ul reaction mixture. Exposure time was 30 minutes.

None of the proteases alone, nor the four in combination, significantly reduced enzyme activity (2 assays done in duplicate). The greatest effect was found with the four enzymes in combination, and they produced an effect (~10% inhibition) that was not statistically significant.

FIGURE CAPTIONS

Figure 1. Mono(ADP-ribosylation) was monitored by following the release of nicotinamide from NAD. The HPLC method was used, as described under Methods. The reaction mixture contained tritiated NAD plus unlabeled NAD to give final concentrations of 10^{-6} to 10^{-3} M. The figure illustrates a representative experiment done with 10^{-5} M NAD and 10^{-8} M toxin. Within the limits of resolution of the assay, there appeared to be a stoichiometric relationship between loss of NAD and appearance of nicotinamide.

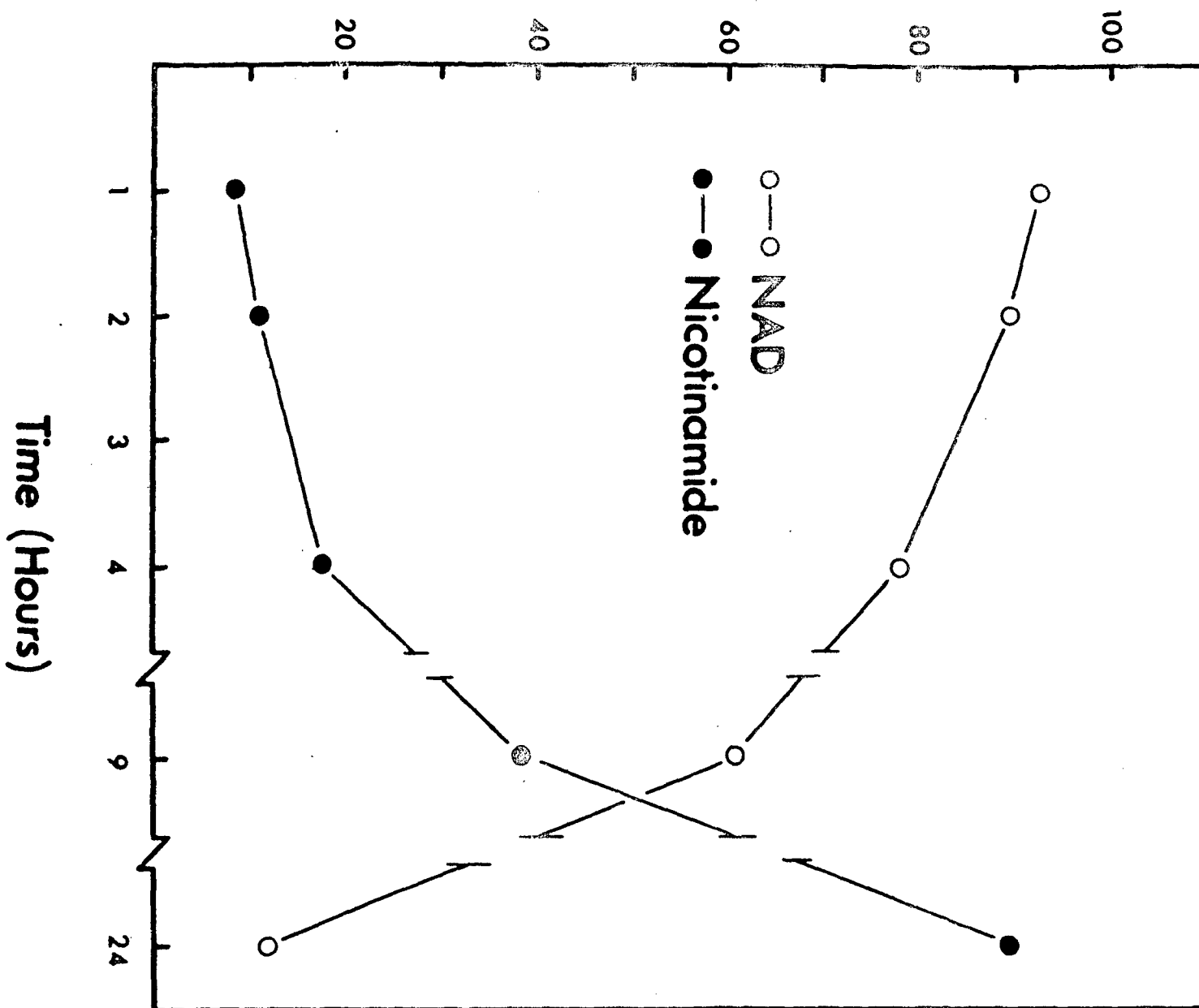
Figure 2. Enzyme activity was measured at various pH values; boric acid-citric acid-phosphate (CBP) buffer and dimethylglutaric acid (DMG) buffer were used. Enzyme activity was measured at 10^{-9} to 10^{-7} M. The figure illustrates a representative experiment done at a concentration of 10^{-8} M.

Figure 3. ADP-ribosyltransferase activity was monitored by following the incorporation of label into homopoly-L-arginine, as described under Methods. Enzyme activity was measured in the absence of added cations or in the presence of individual cations, as indicated. Enzyme activity in the absence of added cations (or in the presence of EDTA, see text) was the same as that in the presence of 1.0 mM cation. However, as the concentrations increased,

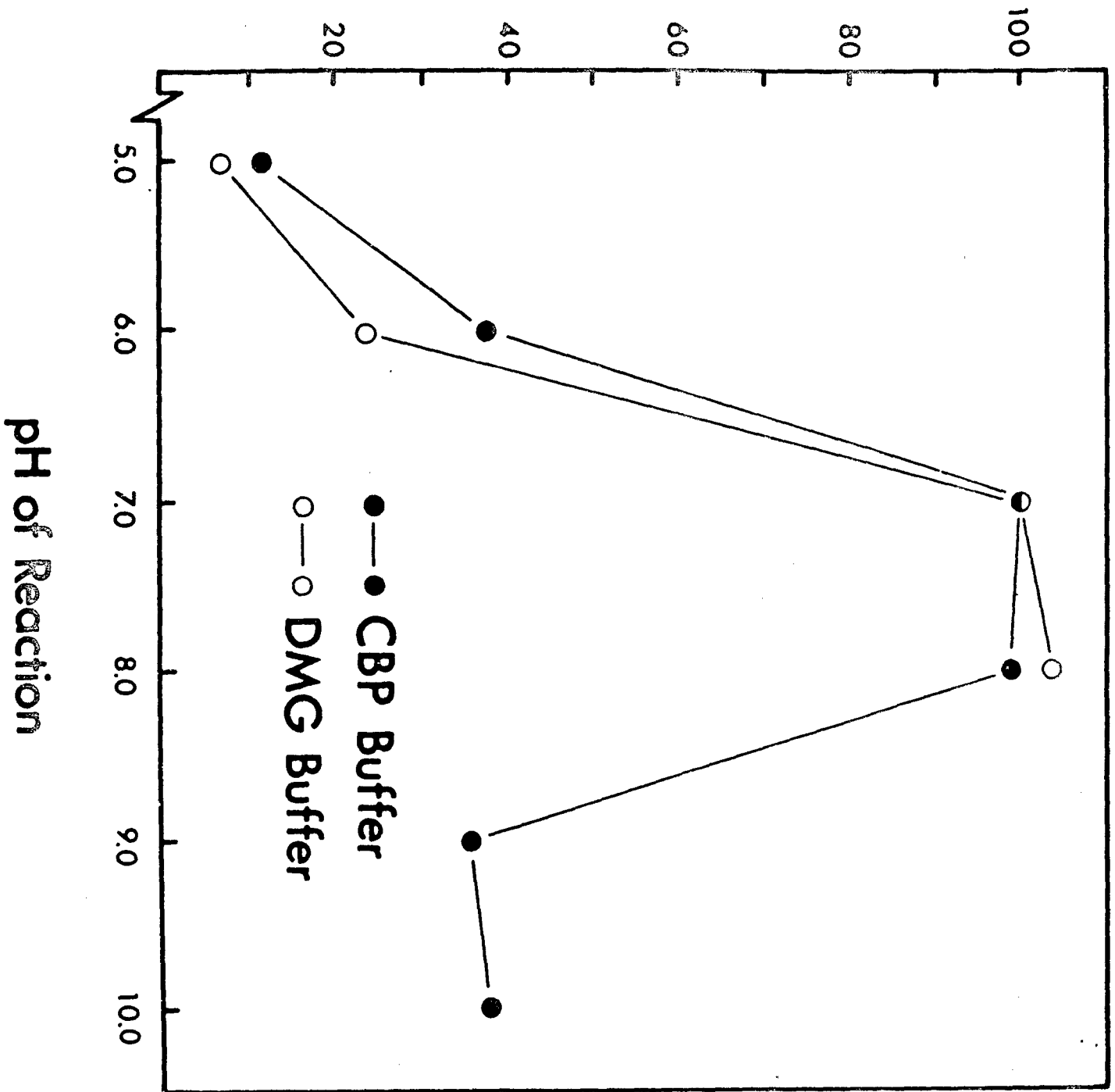
the enzyme activity decreased. Each data point is the mean of three experiments done in duplicate.

Figure 4. Enzyme activity was assayed in the presence of various concentrations of lysolecithin or histone. Both substances enhanced the ADP-ribosyltransferase activity of the toxin (10^{-8} M). Each data point is the mean of three experiments done in duplicate.

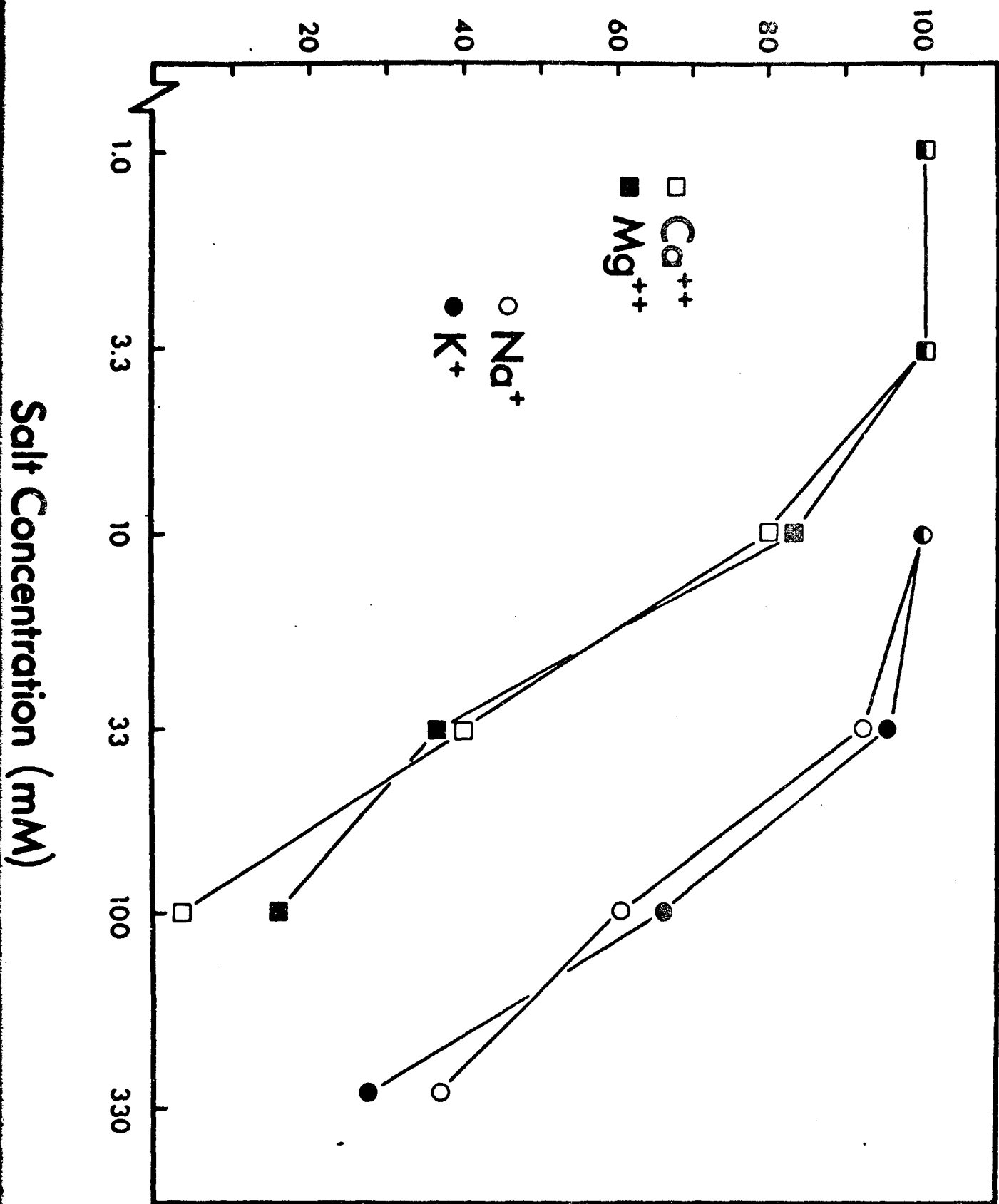
Amount (Percent of Maximum)



Activity (Percent of Maximum)



Activity (Percent of Maximum)



Activity (Percent of Maximum)

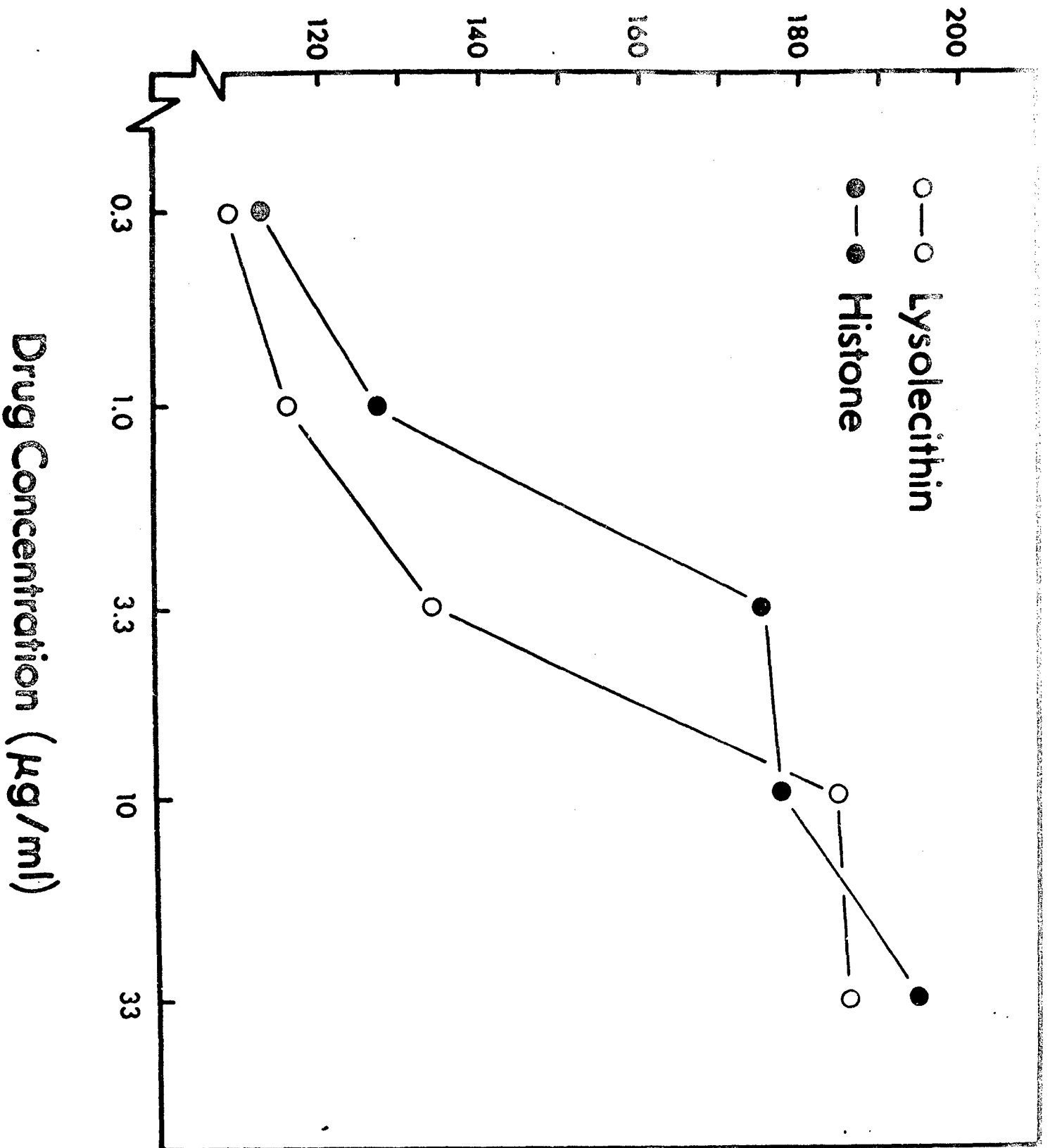


Figure 4

B. Morphology and Messenger Correlates

Specific Aims

1. To develop the adrenal Y-1 cell line model to study the morphological and functional effects of toxins of biological interest.
2. To characterize the action of clostridial binary toxin (C21-C211) (BBT), cholera toxin, Iota and Iota-like toxin on adrenal Y-1 cell morphology.
3. To investigate the effect of BBT, cholera, Iota and Iota-like toxins on adrenal Y-1 cell cAMP and cGMP levels and the response of these cells to the trophic hormone adrenocorticotropin (ACTH).
4. To determine whether there is any correlation between the morphological effect of the various toxins and the adrenal Y-1 cell steroid hormone secretion under basal as well as ACTH-stimulation.
5. To determine the effect of these toxins on adrenal Y-1 cell viability as measured by nucleic acid recovery and ¹⁴C-leucine incorporation into protein.
6. To confirm the BBT-induced ADP-ribosylation of actin in Y-1 cells.

Methods

Cell culture. Y-1 mouse adrenal tumor cells were obtained from American Type Culture Collection (CCL-79) at passage 48 and maintained in Hams F-10 medium with 10% fetal bovine and 2.5% horse serum. Experiments were performed in six well culture plates at 50% confluency. For treatment

with toxins, the medium was replaced with fresh medium without serum containing the concentrations of toxin indicated.

Cyclic AMP and cyclic GMP were measured following 4-6 hour toxin pretreatment. Following toxin pre-exposure the medium was removed and replaced with serum free medium containing 1mM isobutylmethylxanthine (IBMX) to inhibit phosphodiesterase activity. For the determination of cAMP levels the cells were incubated 20 min in the presence or absence of 10mU/ml ACTH. Thereafter, the medium was removed and the cells extracted with 50% acetic acid and assayed for cAMP as described by Sherwin and Tong, 1975.

For the determination of cGMP the cells were incubated 1h in the presence or absence of 100 nM atrial natriuretic factor (ANF). The cells were then extracted with 6% trichloroacetic acid (TCA) for measurement of cGMP. cGMP was assayed by radioimmunoassay (cyclic GMP [125] I RIA KIT, New England Nuclear, Boston Ma.) following acetylation.

To determine the effect of toxins on steroid hormone output the growth medium was replaced with fresh Ham's F-10 without serum and containing the toxins in the concentrations indicated. The cells were incubated 24h and the medium removed for assay of steroid hormones.

Cell cytosol and membrane fractions were prepared by sonication of freshly detached cells in 50mM triethanolamine HCl, pH 7.4, containing 1mM EDTA and 0.05 mM phenylmethyl sulfonyl flouride. The resulting sonicate was centrifuged

at 105,000 xg in a Sorvall RC60 ultracentrifuge for 60 min. The supernatant is taken as cell cytoplasm. Alternately, the cell sonicate was centrifuged at 30,000xg for 15 min and the resulting supernatant used as a crude membrane fraction.

Steroid hormone assay. Secreted adrenal steroids were extracted from the incubation medium and assayed by the fluorometric method of Kowal and Fiedler, (1968) as modified by Temple and Wolff, (1973). Briefly, 0.5 ml of the medium was extracted in 2.5ml of methylene chloride, and washed once with 0.5ml of 0.1N NaOH. One ml of the organic phase was reacted with 1.5ml of 65% sulfuric acid in ethanol (95%). Following mixing, the fluorescence of the acid-ethanol extract was determined at an excitation wave length of 470nm and emission wave length of 530nm in an Aminco-Bowman spectro-fluorometer. (American Instruments, Silver Springs, MD)

DNA determination. Cell DNA levels were determined in aqueous cell extracts using the technique described by Cesarone et al., 1979. Cell extracts (0.4ml) are added to 2.0ml of 2 M NaCl, 50mM NaH₂PO₄, pH 7.4. To this was added 2 g bisbenzimidazole (Hoechst 33250 Sigma Chemical Co., St. Louis, MO.) and the reaction allowed to proceed at least 90 min. Fluorescence was then determined at 458nm with excitation at 356 nm in an Aminco-Bowman Spectro-fluorometer. Calf thymus DNA (Sigma Type I) was employed as a standard.

Leucine incorporation into protein. Leucine incorporation into TCA-precipitable protein was measured as described by Sherwin and Tong, (1976). Briefly, cells were preincubated with cholera toxin (1×10^{-10}) or BBT (1×10^{-9} M) for 22h. The medium was then replaced with fresh Hams F-10 serum media supplemented with 50mM leucine containing 0.2 Ci/ml 14 C-leucine. After 2h of incubation the medium was removed and the cell protein precipitated with 6% TCA, washed with ethanol, ethanol-ether (50:50, V:V) and ether. The resulting pellet was then redissolved in 0.3N KOH. Aliquots were taken for protein determination by the method of Lowry, and for determination of 14 C-leucine activity by liquid scintillation spectrometry. Protein synthesis was expressed as dpm/mg DNA/2h.

Results

Toxin-induced cell rounding in adrenal Y-1 cells. As shown in Fig. 1, addition of ACTH (10mU/ml) caused a rapid rounding of the mouse adrenal Y-1 cell line. This rounding can be seen within minutes and involves all cells within 1h. Rounding of the Y-1 cells is also induced by cholera toxin (1×10^{-10} M). In contrast to ACTH, the onset of rounding was delayed 30-60 min and was not complete until nearly 5h of exposure. BBT (10^{-9} M) also induce cell rounding which like cholera exhibited a lag phase of about 30 min but was complete within 4h. In contrast, neither Iota toxin, Iota-like toxin (data not shown) nor E. coli endotoxin (data not shown) had any apparent effect on cell morphology. As had

been shown previously by this laboratory the morphological changes induced by ACTH, cholera toxin and BBT do not correlate with the effect of these agents on intracellular cAMP. Thus, in contrast to ACTH or cholera, BBT had no effect on either basal or ACTH-stimulated cAMP accumulation in adrenal cells.

As shown in Figure 2, neither cholera, BBT nor Iota toxin had any effect on basal or ANF-stimulated cGMP levels in the Y-1 cells. Basal cGMP concentration in the Y-1 cell were extremely low (5-6 fmol/mg DNA) which is near the limit of sensitivity of the assay system used. However, ANF is a potent stimulator of cGMP levels, and a toxin effect on guanylate cyclase, either stimulatory or inhibitory, would have been expected to be demonstrated by a potentiation or attenuation of the response to ANF, respectively.

Toxin mediated changes in steroid secretion. We had reported in an earlier report that BBT had an inhibitory effect on ACTH-stimulated steroid hormone output. However, analysis of this data suggested that the Y-1 cell variant used in these experiments had not been the same as that routinely used. Therefore freshly thawed Y-1 cells were explored for the effect of toxins. As shown in Fig. 3, treatment of Y-1 cells with BBT ($1 \times 10^{-9}M$) for 24h did result in a significant increase in steroid hormone production. As expected, ACTH and cholera were also effective, while Iota toxin was without effect. Their findings are compatible with the previous findings if we assume that BBT exerts an

effect on steroid hormone release through a mechanism similar to that of ACTH or cholera but of a site post cAMP generation. Experiments are currently underway to explore the synergistic/antagonistic interaction between ACTH and BBT on steroid secretion.

Effect of BBT on nonmorphological indices of adrenal cell function. In order to ascertain whether BBT treatment of adrenal Y-1 cells resulted in irreversible damage and subsequent lysis, two approaches were utilized. First, DNA recovery from tissue culture cells was analyzed from two series of experiments; both included a 24h pretreatment of the Y-1 cells with ACTH (10mU/ml) BBT (1×10^{-9} M) or cholera (1×10^{-10} M). In one series the cells used were at 50% confluency (n=10) and in the other at 100% confluency (n=4). In neither series did the amount of DNA/well vary within or between any of the experimental/or control groups. Thus, at 100% confluency the DNA recovered after 24 hours of treatment was 24 ± 3.0 mg/well for control, nontoxin treated cells; 30 ± 3.6 mg/well for ACTH treated, 30 ± 3.5 mg/well for BBT-treated and 31 ± 3.1 mg/well for cholera treated cells.

In a second set of experiments we explored whether BBT treatment of the Y-1 cells resulted in any impairment in protein synthesis. Y-1 cells were pretreated for 22h with either no additions, 10mU/ml ACTH, 1×10^{-9} M BBT or 1×10^{-10} M cholera. Thereafter, the medium was removed and replaced with fresh medium containing radiolabeled leucine, and leucine incorporation into protein obtained as described in

Methods. In 4 separate determinations control incorporation was 650 ± 46 dpm/mg DNA, 682 ± 15 dpm/mg DNA for ACTH treated cells, 645 ± 83 dpm/mg DNA for BBT treated cells and 449 ± 28 dpm/mg DNA for cholera treated cells. These results suggest that a 22 hour exposure of the cells to BBT does not result in any significant impairment in protein synthesizing capacity. However, cholera toxin treatment may result in some degree of compromise in protein synthesis in these cells.

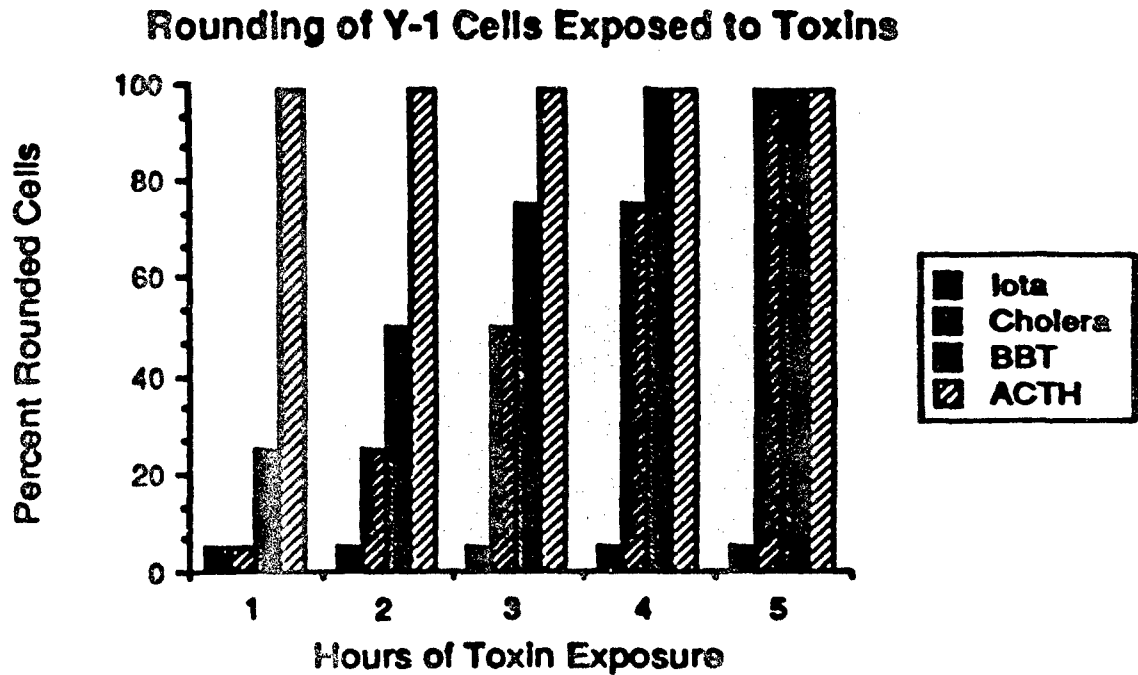


Figure 1 Rounding of Y-1 cells exposed to toxins. For observation of cell morphology, growth medium was removed and replaced with fresh serum medium. Toxin was applied to duplicate wells and rounding scored as the average number of cells rounded per four random fields of 25 cells each. The concentrations of agents treated were; ACTH, 10mU/ml; cholera toxin, $1 \times 10^{-10}M$; BBT, $1 \times 10^{-9}M$.

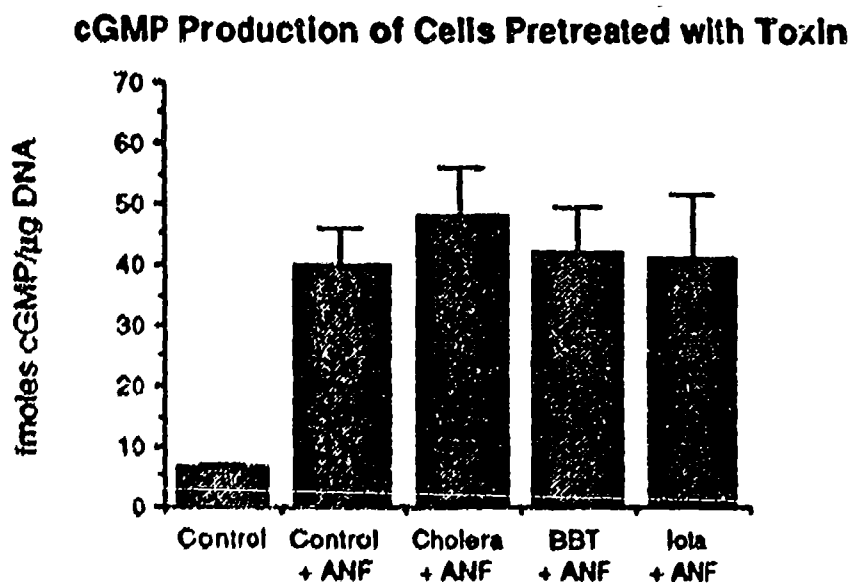


Figure 2 Effect of toxin pretreatment on ANF-stimulated cGMP accumulation in adrenal Y-1 cells. Cells were pretreated with the toxins indicated for 4-6 h then assayed for the stimulatory effect of ANF ($1 \times 10^{-9}M$) on intracellular cGMP. Concentrations of toxins employed were: cholera, $1 \times 10^{-10}M$; BBT, $1 \times 10^{-9}M$; and Iota, $1 \times 10^{-10}M$. Mean \pm SEM of 4 separate experiments.

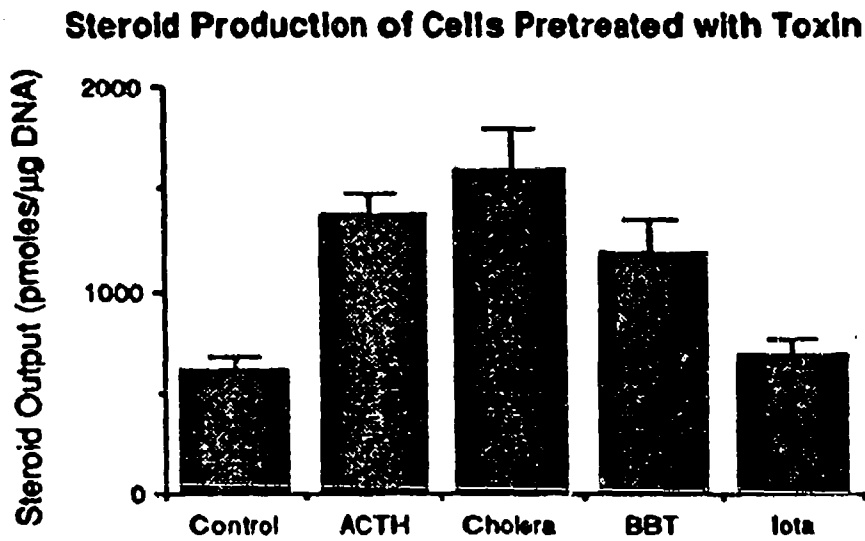


Figure 3 Effect of addition of various toxins and ACTH on the 24h steroid output of adrenal Y-1 cells. Cells were incubated with the toxins or ACTH (10mU/ml) for 24h and the steroid content of the medium assayed. Concentrations: Cholera, $1 \times 10^{-10} \text{M}$; BBT, $1 \times 10^{-9} \text{M}$; and Iota, $1 \times 10^{-7} \text{M}$. Values represent mean \pm SEM of at least six separate experiments.

III. Electrophysiological Studies

A. Pyrethrins

Specific Aims

The sodium (Na^+) channel is a voltage-sensitive transmembrane protein which is important in nerve and muscle impulse conduction. This protein changes its conformation (state) when intracellular voltage becomes more positive. In one conformation, the channel opens, forming a pore through which Na^+ ions can flow into the cell. Among the toxic substances which have evolved to alter Na^+ channel function are the pyrethrins, which protect some Chrysanthemum species from insect infestations. The pyrethroids are synthetic analogs of the pyrethrins.

The goals of the study on low molecular weight neurotoxins are to determine the mechanisms by which pyrethroid insecticides prolong Na^+ channels in the open configuration. This will be done by examining the activity and kinetics of normal and pyrethroid-modified Na^+ channels at the molecular level as described below in Methods.

Methods

The present studies investigate the activity of individual

Na^+ channels using mouse neuroblastoma N1E-115 cells, which are easy to maintain in tissue culture and from which recordings of Na^+ current passing through single open Na^+ channels are readily obtained.

The technique used to record Na^+ channel activity is called the patch clamp technique. To obtain patch clamp recordings, a glass patch pipette will be made by heating and pulling glass capillary tubes to produce pipette tips having inner diameters $\leq 1 \mu\text{M}$. The patch pipette, filled with an external solution designed to record only Na^+ currents (in mM: NaCl 140, CsCl 5, CaCl_2 1.8, MgCl_2 0.8, and HEPES 5 pH 7.3) was placed on the cell surface using a micromanipulator. Slight suction was applied to the pipette, causing a tight mechanical seal to be formed between the pipette tip and the cell membrane. Current recordings were made from the individual (single) Na^+ channels which were contained in the membrane patch. When a channel opened, the flux of Na^+ ions passing through the channel was sensed by the electrical recording apparatus to which the pipette was connected. To control the ionic composition of internal in addition to the external solutions as well as the exact voltage across the cell membrane, membrane patches were excised away from the cell. To do this, the cell membrane outside the patch was made weak by perfusing the bath with an intracellular solution having low Ca^{2+} (in mM: CsF 145, NaF 1.4, and HEPES 5, pH 7.0). The composition of this solution was such that only Na^+ channel currents were recorded. After this, the pipette was moved away

from the cell, excising the membrane patch contained in the pipette tip. The isolated membrane patch was in the inside-out configuration in which the cytoplasmic face is exposed to the now appropriate intracellular bath solvent having low Ca^{2+} .

The electrical recording apparatus (the patch clamp) to which the patch pipette is connected controls both the transmembrane voltage and records Na^+ current passing through open Na^+ channels. The resting voltage across the patch was -100 mV, a potential at which both normal and modified Na^+ channels are closed. The energy to open the channels was provided by presenting a positive voltage step to the patch (from -100 mV to -30 mV). Channel modification was performed by exposing the internal (cytoplasmic) face of the membrane patch to the pyrethroid insecticide deltamethrin (MW 505) at concentrations of 10 μM or in trace concentrations as described in the Results. Current recordings from the patch clamp were digitized with an analog-to-digital converter and stored on an IBM PC/AT.

Results

While normal Na^+ channel activity (channel openings and closings) in response to a voltage pulse stimulus ends within at most 10 - 20 milliseconds (ms) after the beginning of the pulse, deltamethrin modified channel activity remains for up to seconds after the pulse onset. A variety of Na^+ channel states are prolonged by deltamethrin (Chinn and Narahashi, 1986). One state

occurs in which the channel repeatedly opens and closes (channel flickering, Fig. 1) and another in which the channel opens once for a prolonged period of time and after it closes, it remains closed (prolonged opening, Fig. 2).

The experiments performed during the last quarter investigate the effect of deltamethrin concentration ([deltamethrin]) and voltage pulse protocol (described in detail later) on the frequency of appearance of the flickering and prolonged open modified Na^+ channel states. The experiments investigating effects of [deltamethrin] on channel states explore the possibility that more than one site of channel modification exists. The experiments investigating the effects of voltage pulse protocol were designed to test whether deltamethrin-modified channels undergo a regular but protracted relative to normal channels, series of conformational changes upon stepping from one voltage to another.

In experiments examining the effects of [deltamethrin] on channel behavior, I found that the type of observed modified open state (flickering vs prolonged open state) was in fact dependent on [deltamethrin]. It is known that unless the bath chamber is washed with DMSO or alcohol, the trace concentrations of pyrethroid that remain can modify squid axon Na^+ channels (Narahashi, personal communication). Therefore, to test the effects of trace concentrations of deltamethrin on single mouse neuroblastoma Na^+ channels, in these preliminary experiments, a

low deltamethrin concentration ($[\text{deltamethrin}] = \text{LC}$) was obtained by first adding 10 μM deltamethrin to the bath followed by complete replacement of the bath fluid with solution free of deltamethrin. The low deltamethrin concentration was due to the residual deltamethrin that was not washed out. A glass coverslip containing neuroblastoma N1E-115 cells was then added to the bath. A dependence on $[\text{deltamethrin}]$ of flickering and prolonged open channel states was found. In a series of voltage pulses, the percent of current traces showing flickering channel events changed from $79 \pm 13\%$ SD ($N=6$ patches) at $[\text{deltamethrin}] = \text{LC}$ to $9 \pm 6\%$ ($N=4$) in 10 μM deltamethrin while for the prolonged open channels the percentages were $21 \pm 13\%$ ($N=6$) at $[\text{deltamethrin}] = \text{LC}$ and $91 \pm 5\%$ ($N=4$) in 10 μM deltamethrin. Such changes were also found in the same patch exposed to $[\text{deltamethrin}]$ at LC and 10 μM ($N=2$).

These experiments indicate that deltamethrin may act at two different sites on the channel, producing distinctly different modified channel kinetics (prolonged openings or flickering). The difference in dose dependence indicates a difference in binding affinity of the sites for deltamethrin, although dose response curves have not yet been established.

Voltage pulse protocol is defined as the voltage pulse sequence (pulse frequency, duration and amplitude) presented to the channel. Two aspects of voltage pulse protocol, pulse duration and pulse frequency, were found to affect the types of

modified channel states which were observed during a series of voltage pulses.

Modified channel activity (% of current traces showing channel openings) examined in the same patch was found to depend on voltage pulse duration. In experiments using [deltamethrin] = LC, decreasing pulse duration increased channel activity by reversibly increasing the percent of flickering traces (500%, N=2) without significantly affecting the percent of fully conducting channel events. In 2 cells exposed to [deltamethrin] = 10 μ M, the number of prolonged opening channel events decreased by $24 \pm 8\%$ when pulse duration was increased from 100 ms to 3 s. Interpulse interval was 6 s for all experiments.

Preliminary experiments also show that voltage pulse frequency affects modified channel activity and the occurrence of specific channel states. In one membrane patch, current traces showing any channel openings were observed in only 10% of the traces using a 6 s interpulse interval and in 84% of the traces using a 3 s interpulse interval. With the 3 s interpulse interval, flickering lasting >40 ms was observed in 70% and prolonged opening channels in 20% of the traces (some traces had both flickering and fully conducting channels). Flickering was observed in only 4% and prolonged opening channels in 6% of the traces when using 6 s interpulse interval. [Deltamethrin] = LC, 100 ms pulse duration for both frequencies.

These experiments indicate that the channels have a memory for the voltage pulse protocol which lasts for up to several seconds. This is consistent with the idea that deltamethrin stabilizes a number of channel states and that the time required to pass to different states after presenting a voltage pulse occurs on a scale of hundreds of milliseconds to seconds. The modified channel states observed during a pulse depend upon the states that the channel passed through previously, which in turn depend upon the voltage pulse protocol.

References

Chinn, K. and Narahashi, T. 1986. Stabilization of sodium channel states by deltamethrin in mouse neuroblastoma cells. J. Physiol. 380:191-207.

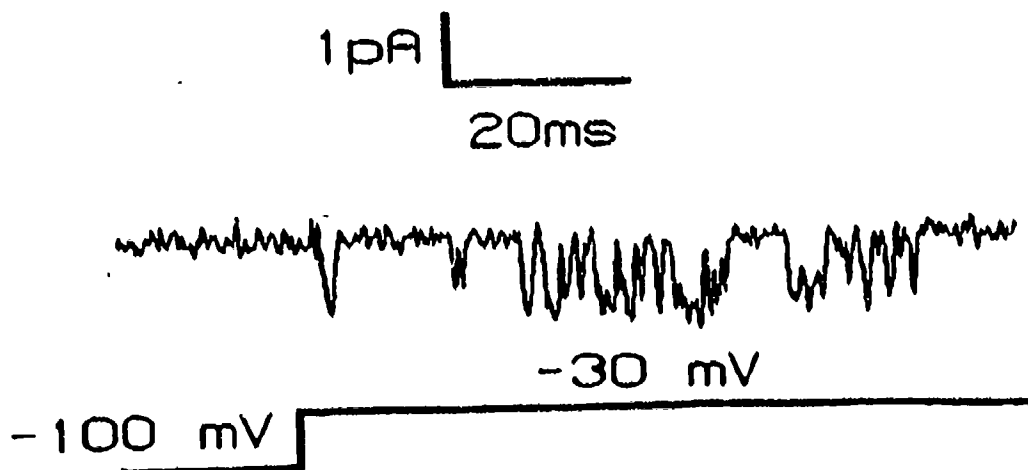


Fig. 1. Current trace showing an individual deltamethrin-modified Na^+ channel flickering between the open and closed state in response to a voltage pulse shown at the bottom of the Figure. Channel openings are depicted as downward deflections of the membrane current. The number of channels in this membrane patch was 3, as determined by the maximum number of simultaneous channel overlaps during a large voltage pulse (to +30 mV). The flickering behavior therefore cannot be explained by consecutive openings of dozens of different channels.

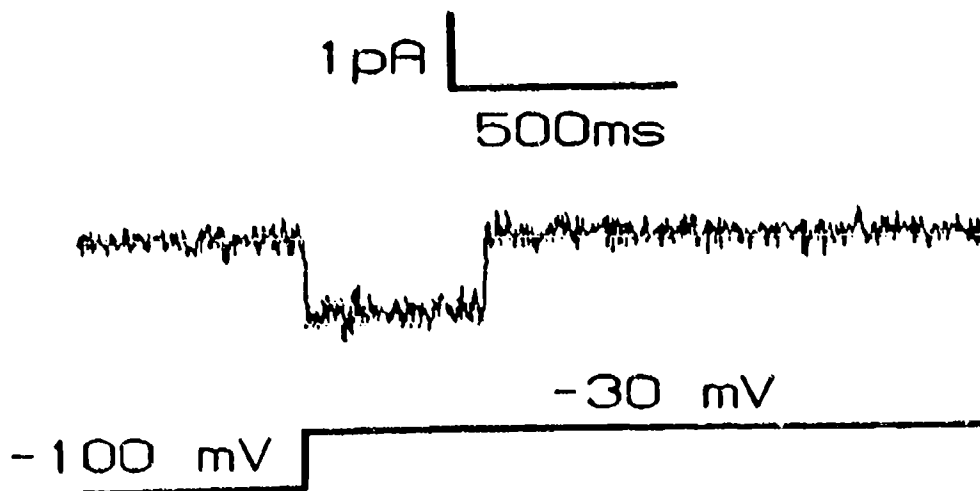


Fig. 2. Current trace showing a prolonged opening of a deltamethrin-modified Na^+ channel. The voltage pulse stimulus is shown at the bottom of the Figure.

B. Ryanodine

Specific Aims:

The objectives of these studies are to determine the sites of action of ryanodine on fast skeletal muscle fibers in relation to the pharmacodynamic action of ryanodine. This report represents a summary of our findings to date.

Methods:

The isolated frog sartorius muscle is composed of fast glycolytic muscle fibers that run in parallel from the tendon connection at the pubic symphysis to the tendon attachment at the knee of the frog. The structure of the amphibian type muscle fiber is shown in Fig. 1. The paired muscles are dissected and mounted in a circulating chamber that allows for temperature control and easy change of bathing solutions. The distal tendon is attached to a chain that allows for tension recording and the proximal end is anchored to a glass holder in the chamber. Tension is recorded as a function of ryanodine concentration and time of exposure. Tension in fast muscle fibers develops at a threshold concentration of 5×10^{-7} M free calcium in the sarcoplasm. The source of calcium is from the terminal cisternae of the triadic junction between the transverse tubules and the sarcoplasmic reticulum. The major source of energy utilization during contraction in fast glycolytic muscle fibers is derived from glycolysis. When muscles are depolarized by potassium between 7 mM K_o^+ and 20 mM K_o^+ the muscle responds by increasing oxygen uptake. The energy sink that is turned on is related to

calcium influx through voltage dependent channels in the sarcolemma and calcium extrusion or uptake by a calcium ATP'ase present both in the transverse tubular junctional membrane and in the terminal cisternae and longitudinal membrane of the sarcoplasmic reticulum. At a K_o^+ level of 2.5 mM the resting calcium activity in the sarcoplasm is $1 \times 10^{-7} M$; at 20 mM K_o^+ the level reaches a threshold level for contraction of $5 \times 10^{-7} M$. Increased oxygen uptake is associated with this increase in calcium activity. Agents that block calcium influx through the voltage dependent channels also block the increased oxygen uptake. Caffeine acts on channels in the terminal cisternae to increase the leak of calcium from the terminal cisternae. These channels are either calcium operated release of calcium channels or receptor operated channels. At low concentrations of caffeine calcium is released to the sarcoplasm and the Ca^{2+} ATP'ases are activated, leading to an increase in oxygen uptake. The calcium concentration in the sarcoplasm is greater than $1 \times 10^{-7} M$ and less than $5 \times 10^{-7} M$.

The measurement of oxygen consumption in muscle is a very sensitive indicator of the rise in calcium activity in the sarcoplasm below the threshold for contraction.

A special chamber consisting of glass or lucite walls and containing a sealed oxygen electrode facing the inner wall of the chamber is used to measure oxygen uptake. The muscle is mounted on a special holder and placed in the chamber; the bathing solution is rapidly vortexed by a magnetic stirrer at the base of the unit. Rapid flow of the solution across the surface of the oxygen electrode is essential for accurate measurement of oxygen uptake by the muscle.

The whole unit is placed in a constant temperature bath that allows for good temperature control. The barometric pressure is recorded and μl of oxygen uptake is converted to $\mu\text{mol O}_2 \text{ g}^{-1} \text{ hr}^{-1}$.

⁴⁵Ca Efflux Studies: The muscles are dissected and equilibrated in oxygenated physiological salt solution for 60 minutes. After 60 minutes equilibration the muscles are placed in ⁴⁵Ca PSS ($\mu\text{Ci/ml}$) for 3 to 4 hours. The muscles are then rinsed by 4 quick dips in non-radioactive PSS and then placed in a washout chamber containing 3 ml of PSS. Collections are made every five minutes. After 80 minutes washout of the extracellular and fast exchanging calcium, ryanodine is added and washout continued to 130 minutes. The control muscle receives no drug during ⁴⁵Ca washout.

Results: Ryanodine contracture

1. The effect of replacement of sodium by choline to block Na^+ for Ca^{2+} exchange across the sarcolemma on ryanodine induced contracture in muscle.

The threshold concentration of ryanodine required to cause a contracture in resting muscle is 10^{-4}M after a latent period of 30 minutes and a time to half peak tension of 60 minutes. Table 1 shows that replacement of sodium by choline lowers the concentration of ryanodine to cause a contracture from 10^{-4}M to 10^{-6}M and reduces the half time to peak tension from 60 min to 40 min.

2. The effect of ryanodine on oxygen uptake is shown in Table 2 along with the inhibition of ryanodine stimulated oxygen uptake by benzocaine. Benzocaine, a non-charged local anesthetic known to block caffeine induced release of calcium from the sarcoplasmic reticulum also blocks the increase in oxygen uptake. Peak oxygen

uptake is achieved 5 minutes after the addition of ryanodine to the physiological solution bathing the muscle and then returns to base line by 20 minutes. Figure 2 shows the time course for development of peak oxygen uptake at 10^{-10} M. Figure 3 shows that ryanodine at 10^{-8} M causes a rapid increase in ^{45}Ca efflux which reaches a peak within five minutes and declines back to baseline in thirty minutes. The increased efflux correlates well with the increased oxygen.

The increased oxygen uptake and release of calcium from the terminal cisternae of the sarcoplasmic reticulum occurred without any increase in tension indicating that the ionized calcium level had risen from a basal level (1×10^{-7} M to a subthreshold level for contraction of 5×10^{-7} M).

The transverse tubular element of the sarcolemma can be uncoupled from the terminal cisternae by treatment of the muscle with 400 mM glycerol for 60 minutes, followed by 60 minutes recovery in normal PSS solution. The hyperosmotic shock (sarcoplasm hypertonic to normal PSS) causes swelling and disruption of the t-tubule leading to uncoupling of the muscle action potential from contraction. Table 3 presents the data demonstrating that ryanodine at concentrations below 10^{-4} M no longer enhances oxygen uptake. At 10^{-4} M ryanodine causes nearly a six-fold increase in oxygen uptake. Benzocaine blocks the increase in oxygen uptake. The loss of the high affinity receptor site for ryanodine by glycerol shock treatment indicates that the high affinity receptor site is located in the transverse tubular element.

Recent studies (Lai et al., Campbell, et al.) indicate that the junctional feet between the transverse tubule and the terminal cisternae form a ryanodine receptor complex. The junctional feet are believed to regulate, or are part of the calcium release channel associated with excitation-contraction coupling in skeletal muscle. Ryanodine at low concentrations opens these channels which appear to inactivate (see Fig. 2) and cause sufficient calcium release to increase the activity of the Ca-ATP'ase in the sarcoplasmic reticulum and hence increase oxygen uptake to maintain the necessary level of ATP and creatinine phosphate in muscle.

There are three fundamental proposals for the coupling of the action potential to calcium release from the sarcoplasmic reticulum (see Fig. 1). The first is the Schneider-Chandler model in which Ca^{2+} release channels are mechanically or chemically activated with a time constant of ≈ 200 usec during the potential change between -50 mV and -20 mV of the action potential. The second proposal is depolarization of the TC membrane with current flow occurring across the junctional membrane at the site of the junctional feet.

The third proposal for excitation-contraction coupling by Bianchi (1968) and Frank (1958, 1982) is that the depolarization of the junctional membrane releases calcium bound on the cytoplasmic side of the junctional membrane to activate calcium release of calcium channels in the terminal cisternae (Miyomoto and Racker, 1981).

Ryanodine, at low concentrations 10^{-11} to 10^{-9} M appears to open a calcium channel in the terminal cisternae; at concentrations

between 10^{-9} and 10^{-6} M ryanodine depresses the skeletal muscle twitch and blocks calcium release of calcium channels in cardiac muscle. At concentrations between 10^{-6} and 10^{-4} M, ryanodine appears to irreversibly open calcium channels in the terminal cisternae and to cause a contracture of muscle.

Ryanodine appears to be a powerful tool in elucidating the mechanism of excitation-contraction coupling in skeletal muscle. Inositol 1,4,5-triphosphate (InsP_3) has been proposed as a possible chemical activator in excitation-contraction coupling (Vergara et al., 1985). The high Q_{10} of excitation-contraction coupling suggests a chemical process in linking the junctional membrane to opening of calcium channels in the terminal cisternae of the sarcoplasmic reticulum.

At low concentrations of ryanodine that increase oxygen uptake and calcium release from the sarcoplasmic without changing membrane potential, the formation of InsP_3 should be detected. Cd^{2+} and Zn^{2+} inhibit the enzyme responsible for deactivation of InsP_3 , i.e. InsP_3 5-phosphatase, and consequently should enhance the release of calcium from terminal cisternae by ryanodine and increase the oxygen uptake.

We propose to study the effect of ryanodine on phosphatidyl inositol turnover and on InsP_3 metabolism in relation to excitation-contraction coupling. The effect of ryanodine on excitation-contraction coupling should help reveal the complex nature of the calcium channels involved in excitation-contraction coupling.

Table 1

Effect of choline replacement of sodium in PSS on
Ryanodine contracture of frog sartorius
muscle

Solution	Peak tension g/g wet wgt	Time to half- peak tension min
NaPSS + 10^{-6} M Ryanodine	no contracture	
NaPSS + 10^{-5} M Ryanodine	"	up to 120 min
NaPSS + 10^{-4} M Ryanodine	26	60
Choline PSS + 10^{-6} M Ryanodine	18	40

The blocking of the sodium calcium exchanger in the sarcolemma block part of the calcium efflux allowing calcium released from the terminal cisternae to reach threshold concentration in the sarcoplasm at a 2-fold lower concentration of ryanodine.

Table 2
Peak oxygen uptake in frog
sartorius muscle in vitro

Ryanodine Conc. M	Oxygen uptake $\mu\text{mol O}_2 \text{ g}^{-1} \text{ hr}^{-1}$	
	- benzocaine	+ 2.5 mM benzocaine
0	2.3	2.5
10^{-11}	23.4	---
10^{-10}	27.1	---
10^{-9}	10.3	---
10^{-8}	10.7	2.3
10^{-7}	11.6	3.7
10^{-6}	10.5	2.4
10^{-5}	12.0	2.4

Table 3

Effect of Ryanodine on O₂ uptake in
glycerol shocked muscles

N	Ryanodine	O ₂ Uptake $\mu\text{mol g}^{-1} \text{hr}^{-1}$
5	0	2.2±0.4
4	10 ⁻⁶ M	2.3±0.2
5	10 ⁻⁵ M	2.4±0.2
4	10 ⁻⁴ M	12.4±0.3
4	10 ⁻⁴ M + 2.5 mM Benzocaine	4.2±0.3

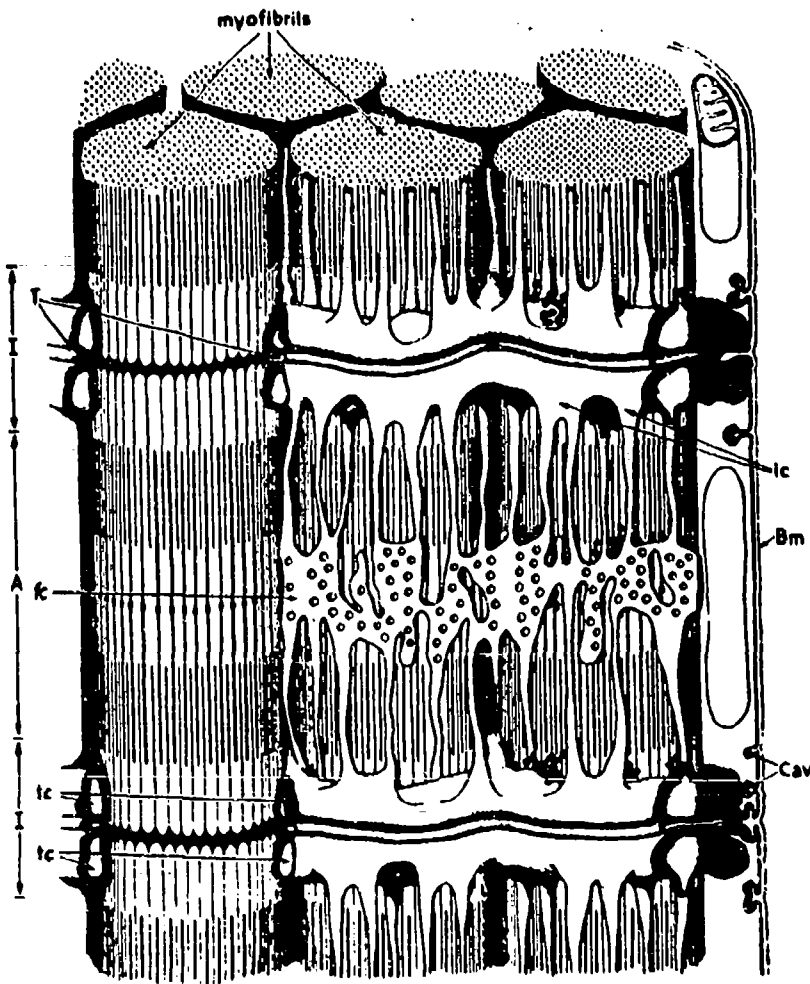


Fig. 1. Transverse tubular system and sarcoplasmic reticulum in frog twitch fibers. Bm, Basement membrane; Cav, caveolae; T, transverse tubular system; fc, fenestrated collar; ic, intermediate cisternae; tc, terminal cisternae; A, A band; I, I band. This figure is an extension of Peachey's well-known drawing of 1965.⁽⁶⁾

The second tubular system, namely the SR, envelops each myofibril and cannot be reached by large extracellular markers. It consists of three main elements: (1) the terminal cisternae (TC) which adjoin and cover the major part of the T system; (2) the intermediate cisternae; and (3) the fenestrated collar (see Fig. 1).

The T system comprises 0.32% of the fiber volume, the TC 4.1%, and the rest of the SR about 5%.^(6,7,14) In a fiber with a diameter of 100 μm , the surface of the T system is about six to nine times larger than the smooth cylinder surface.⁽⁷⁾ This fact and the additional increase in surface area provided by the caveolae, explain the apparently large membrane capacity of 7 $\mu\text{F}/\text{cm}^2$ (referred to the cylinder area) measured in fibers with a diameter of 100 μm .⁽¹⁵⁾

The region in which two TC of the SR and one tubule of the T system come into apposition is called a triad. About 60–80% of the surface of the T system is surrounded by the SR^(6,14) whereby a gap of only 12–14 nm separates the two systems. In part of this region of close association, electron-dense "feet" cross the junctional gap and join SR and T-tubule membranes. They appear as solid structures with electron-opaque interiors and are arranged in a tetragonal disposition (forming two or multiple parallel rows) at a density of 790 per μm^2 of tubular membrane (in frog muscle).^(8,16–18) With different fixation and

staining methods, pillarlike structures instead of feet can be detected.^(19,20) They are defined as pairs of electron-opaque lines bounding an electronlucent interior spanning the gap between the T system and the SR.⁽¹⁹⁾ Under resting conditions, there are 39 pillars per μm^2 of tubular membrane.

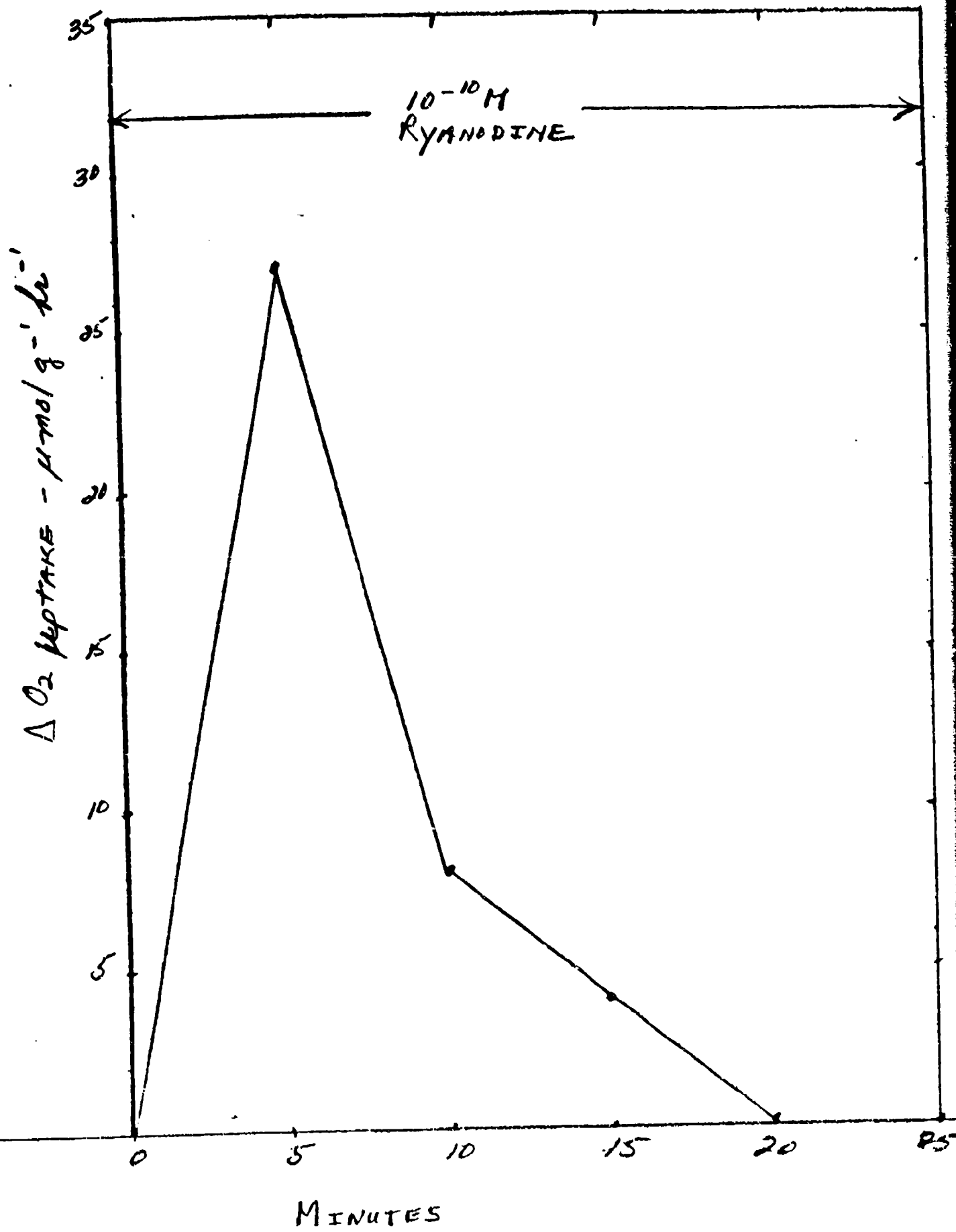
The diversity of the tubular systems in different fiber types from various animals and the correlation between morphology and function have been well covered in two reviews.^(3,8)

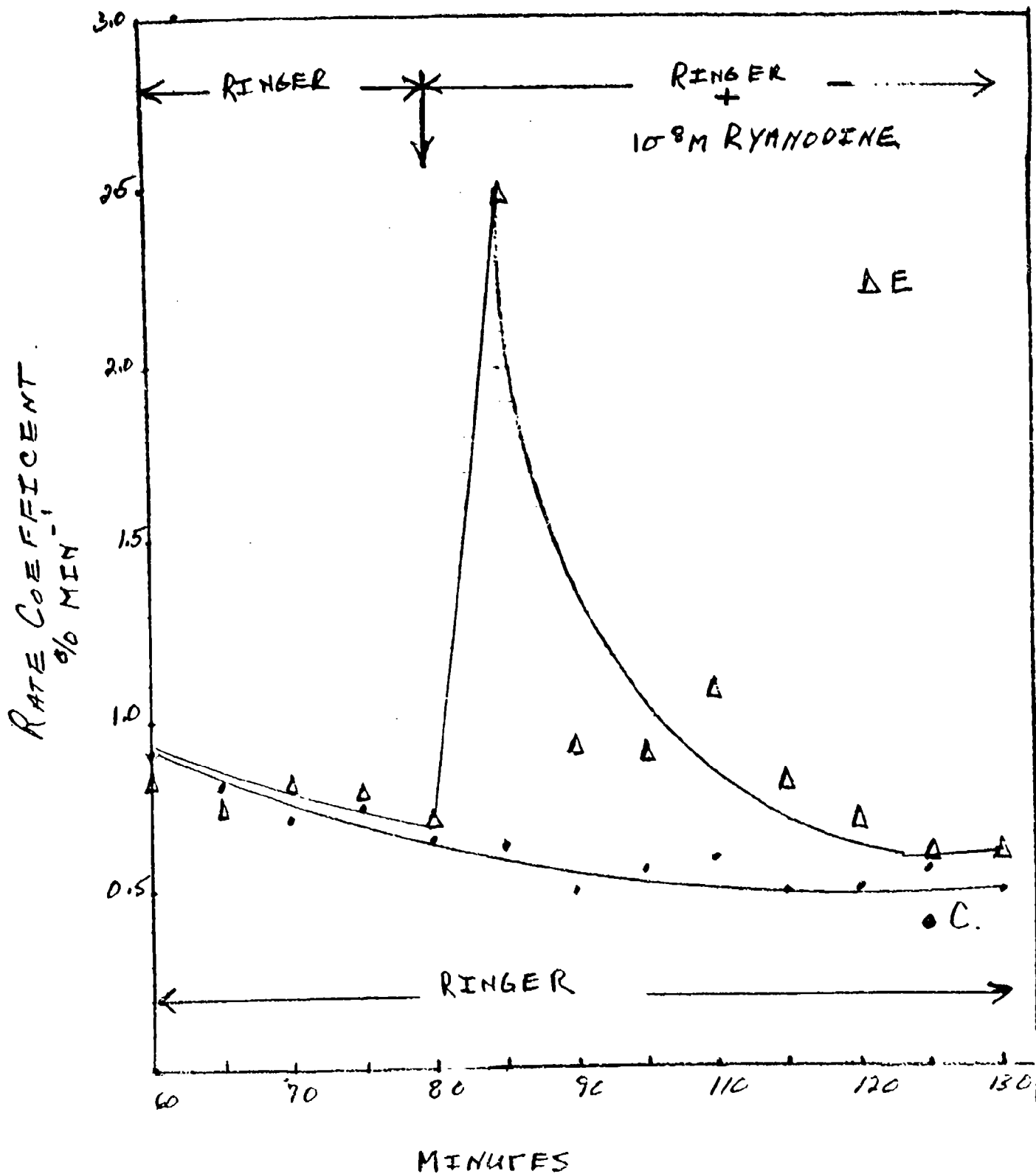
3. Electrical Properties of the Surface and Tubular Membrane

Table I presents the concentrations of the main ions in the extracellular fluid (Ringer's solution) and in the myoplasm of frog skeletal muscle fibers (see Refs. 21 and 22). The data, taken from different publications,^(21–26) may serve as a starting point for the analysis of the origin of the membrane potential during rest and activity in these fibers. In the resting state the membrane is mainly permeable to Cl^- and K^+ ions for which, in a defined concentration range, a Donnan distribution will be displayed. At external K^+ concentrations higher than 10 mM, the membrane behaves like a K^+ or Cl^- electrode if $[\text{K}^+]_o$ and $[\text{Cl}^-]_o$ are

Fig 2

⁻⁵⁸⁻
Effect of Ryanodine on O₂ uptake in frog
Sartorius muscle.





References

- Lai, F. Anthony, Erickson, H., Block, B.A. and G. Meissner. Evidence for a junctional feet ryanodine receptor complex from the sarcoplasmic reticulum. *Biochem. and Biophys. Res. Comm.* 143: 704-709, 1987.
- Campbell, K.P., Knudson, M., Toshiabi, I., Leung, A.T., Sutko, J.L., Kahl, Steven D., Raab, C.R. and L. Madson. Identification and characterization of the high affinity ^3H ryanodine receptor of the junctional sarcoplasmic reticulum Ca^{2+} release channel. *J.B.C.* 262: 6460-6463, 1987.
- Bianchi, C.P. Pharmacological actions on excitation-contraction coupling in striated muscle. *Fed. Proc. Am. Soc. Exp. Biol.* 27: 126-131, 1968.
- Frank, G.B. Inward movements of calcium as a link between electrical and mechanical events in contraction. *Nature* 182: 1800-1801, 1958,
- Frank, G.B. Roles of extracellular and "trigger" calcium ions in excitation-contraction coupling in skeletal muscles. *Can. J. Physiol. Pharmacol.* 60: 427-439, 1982.
- Miyamoto, H. and Racker, E. Calcium induced calcium release at terminal cisternae of skeletal sarcoplasmic reticulum. *FEBS Letters* 133: 235-238, 1981.
- Vergara, J., Tsien, R. and M. Daley. Inositol 1,4,5-triphosphate: A possible chemical link in excitation-contraction coupling. *Proc. Natl. Acad. Sci.* 82: 6352-6356, 1985.